PERGAMON

Carbon 39 (2001) 2247–2268

CARBON

Review article

The oxidation of soot: a review of experiments, mechanisms and models

B.R. Stanmore*, J.F. Brilhac, P. Gilot

Laboratoire Gestion des Risques et Environnement, Université de Haute Alsace, 25, rue de Chemnitz, 68200 Mulhouse, France

Received 8 January 2001; accepted 13 April 2001

Abstract

Soot may be formed when carbonaceous fuels are burned under local reducing conditions. Its subsequent oxidation is of great significance for pollution control in industrial flames, auto engines etc. Oxidation (gasification) can be achieved with oxygen, carbon dioxide, water vapour or nitrogen dioxide. In this review, the experimental techniques which have been used to study the gasification of soot are described and the methods and results obtained by analysis of the data from them are considered. Firstly, the mechanism of soot formation and its structure are briefly discussed. The various scales of particulate which comprise it, i.e. spherule, particle and aggregate, influence its properties and behaviour. Next, the experimental equipment used in the study of its gasification is briefly described. Gasification kinetics at low temperatures are measured either in fixed beds or by thermogravimetry. The apparatus may be operated as a thermally programmed desorption system to identify the species involved. High temperature investigations have been carried out in entrainment burners and shock tubes. The chemistry of soot oxidation is discussed for both non-catalytic and catalytic conditions. The oxidation pathway involves interaction between adsorption and desorption processes, which determine the primary products, the order of reaction and the activation energy. The concensus is that two types of adsorbed surface species are present in uncatalysed combustion. The combustion mechanism of individual spherules is considered in terms of basic property changes. During thermogravimetry, the influence of the competition between reaction and oxygen diffusion in soot beds is analysed. The reaction of catalysed soot displays a different mechanism, as the primary products, the order of reaction and the activation energy all change. The lower activation energy and higher reactivity lead to lower ignition temperatures. Catalysts may be incorporated into the soot spherules by addition to the fuel, or may be added after formation. Two types of contact between the carbon and added catalyst have been identified, ‘loose’ and ‘tight’. Tight catalyst, which has been mechanically ground with the soot, produces more pronounced effects. Finally, the behaviour of soot during gasification by other oxidants, namely H_2O, CO_2 and NO_2 is summarised.

Keywords: A. Soot; B. Gasification, Oxidation; D. Chemical structure, Reactivity

1. Introduction

Soot is produced as an unwelcome byproduct in many practical combustion systems. With internal combustion engines, particularly diesels, it can foul exhaust systems and generate dark exhaust plumes. More significantly, it presents a significant environmental hazard when respired, as it often contains adsorbed PAH. The biological effects of diesel exhaust from a catalytic converter have been reported [1,2]. The finer particle sizes present in ambient air, which are formed during combustion, are responsible for increased mortality [3].

However, in large flames soot can perform a useful function by acting as a radiating agent to promote heat transfer. Because of these diverse implications, the literature on soot is scattered. This article reviews those aspects of the literature which relate to its combustion.

Two temperature ranges are of interest, flame temperatures (over 800°C) at which its formation competes with its oxidation, and low temperatures (300–700°C). The latter are found in diesel exhaust systems, and the controlled

*Corresponding author. Present address: Ecole des Mines d’Albi-Carmaux, Route de Teillet, 81013 Albi Cedex 09, France. Tel.: +33-5-6349-3000; fax: +33-5-6349-3099.

E-mail address: stanmore@enstimac.fr (B.R. Stanmore).

0008-6223/01/$ – see front matter
PII: S0008-6223(01)00109-9

Nomenclature

d	particle diameter (m)
D	diffusion coefficient ($m^2\ s^{-1}$)
e	depth of soot bed (m)
ERE	extended resistance equation
h_m	mass transfer coefficient for oxidant ($m\ s^{-1}$)
k	reactivity on a carbon basis ($kg\ kg^{-1}\ s^{-1}$)
K	reactivity on an oxidant basis ($kg\ m^{-3}\ (kg\ m^{-3})^{-1}\ s^{-1}$)
n	order of reaction (–)
P	partial pressure of oxidant (Pa)
RVVR	reactor to visualise and video regeneration
x	displacement into bed from the surface (m)
y	mass fraction of oxidant (–)
u	extent of carbon burnout (–)
α	exponent in ERE equation
β	stoichiometric coefficient ($kg_{ox}\ kg_{carbon}^{-1}$)
ϵ	porosity (–)
θ	Thiele modulus (–)
σ	density ($kg\ m^{-3}$)
ω	flux of oxidant ($kg\ m^{-2}\ s^{-1}$)

Subscripts

a	adsorption
b	bed
d	desorption
e	effective
g	gas
o	initial
ox	oxidant
p	spherule
s	surface

oxidation of particulate emissions using regenerative traps must be initiated in this range. Where possible, the discussion will refer to soot behaviour, with some mention of other turbostratic materials if necessary.

Gasification by CO_2 and H_2O will also be briefly considered. Recent developments in the control of automotive diesel emissions have raised the possibility of using nitrogen dioxide NO_2 as a soot oxidant. It is more reactive than oxygen at low temperatures and is the focus of ongoing research. The C–NO_2 reaction will be therefore be included in the discussion.

In order to interpret combustion behaviour it is necessary to understand the structure and hence the formation mechanism of soot. A brief description of each of these follows.

2. Formation of soot

The term soot is given to the particulates formed during combustion of carbonaceous fuels under substoichiometric conditions, either by design e.g. for the production of carbon black, or in poor mixing conditions (e.g. diesel soot). There is a huge and rapidly growing literature concerning its formation and growth in flames, and only a brief summary is necessary here.

Some older reviews of the topic are still useful and should be consulted, for example [4–7]. A volume of workshop papers is available [8]. The influence of engine operating conditions on the properties of diesel soot has been described [9].

It is universally accepted that sequential nucleation, growth and coagulation steps take place. Soot inception begins in a laminar diffusion flame for a range of hydrocarbons at temperatures between 1585 and 1700 K [10]. It appears that uncharged radicals and molecules are the flame nucleation precursors, i.e. nucleation units [11]. Growth by addition of gaseous carbonaceous species then produces the particles which are comprised of the spherules described in the next section. The particles coagulate into aggregates as the combustion gases cool.

Many mechanistic models for describing speciation and soot formation in flames are available [12]. Acetylene and PAHs appear to supply the bulk of the carbon later incorporated into the soot spherules. Krestinin [13] postulates that polyynes ($C_{2n}H_2$, $n=2, 3, \ldots$) are the major precursor radicals, partly because their stability increases with temperature.

With solid fuels, e.g. coal, soot is formed by the

pyrolysis of tarry materials ejected by particles undergoing devolatilisation. The droplets dehydrogenate and/or partially oxidise into chains of soot spherules. Most are burned before exiting the flame region, but a significant residual can be found in the flyash of low NO_x burners [14].

The soots from various sources, i.e. from different fuels and combustion conditions tend to be similar in size and composition, which indicates that the same formation processes and growth constraints apply. This has encouraged researchers to produce soot for study in simple laboratory combustors [15], or to use commercial carbon black as a surrogate [16,17].

3. Composition and structure of soot

The nature of soot has been discussed at length in previous reviews, see for example Ref. [7].

The ultimate analyses of a typical diesel soot and the same material degassed at 13 mPa for 5 h at 150°C [16] are given in Table 1.

The sulphur was apparently present as compounds adsorbed onto the surface (as sulphates), whereas the oxygen was strongly bonded. FTIR analysis revealed the presence of C=O, C–O–C and C–OH bonds, and some aromatic structures. The unaccounted-for mass in Table 1 is probably in the form of silicon, aluminium and metals.

Soot as sampled, e.g. from a dilution tunnel, is found to be in the form of agglomerates which are around 100 μm in size. These agglomerates are composed of smaller, very open 'particles', which are in turn a collection of smaller carbonaceous spherules. The terms agglomerate (100 μm typical size), particle (0.1–1 μm) and spherule (10–50 nm) will be used for these three scales of particulate. Fig. 1 is a micrograph of some typical particles, showing the individual spherules.

The agglomerates are readily disaggregated into particles by treatment in an ultrasound bath [16]. The mechanism of cohesion is surface forces to which adsorbed materials play a part. The method of sampling influences the morphology, because of different conditions during the coagulation process.

The fundamental unit of the soot agglomerates are the spherules with diameters of 10–50 nm [18]. As the name implies, most of these particles are almost spherical, but a number of less regular shapes may be found. The surface of the spherules has adhering hydrocarbon material or soluble organic fraction (SOF) and inorganic material (mostly sulphates). Ahlström and Odenbrand [19] found that on heating a diesel soot at a rate of 10 K min^{-1}, hydrocarbons were lost in the range 150–400°C, with a pronounced peak at 200°C. Courcot et al. [20] tested a highly impregnated soot and found three distinct hydrocarbon peaks.

Table 1
Typical soot analyses

Element	C	H	N	O	S
Virgin soot	83.5	1.04	0.24	10.5	1.13
Degassed soot	83.8	0.85	0.22	10.7	0.10

The SOF and other adsorbed species such as sulphates and water are captured by the soot in the gas cooling phase e.g. in the exhaust pipe of a diesel engine [21]. The quantity of SOF is a function of engine operating conditions, and may be as low as 5% (loaded engine) or as high as 60% (engine idle) of the total mass. The sample analysed above contained little SOF. The mass loss during solvent extraction (SOF) is almost the same as the mass lost by thermal treatment under inert gas to 600°C [22]. Both lubricating oil and unburned fuel contribute to the SOF of diesel soot [23,24].

The spherules are joined together by shared carbon deposition to form loose particles of 0.1–1 μm size. The nitrogen BET area of a soot was found to be only 40% of the external surface area calculated for spherules whose diameter was measured by electron microscopy [25]. Though the porosity of these particles may be of the order of 0.95, they cannot be broken down into the individual spherules, even by strong ultrasound treatment [16].

Viewing of the spherules by electron microscopy reveals laminations with surface steps, which are produced by numerous crystallites in concentric orientation [7]. The form of the BET adsorption isotherms can give information about the degree of surface defects [26], because of high energy sites at the edges.

X-ray diffraction indicates that the structure of the crystallites has an inter-layer spacing of 0.36–0.35 nm [23,27], i.e. slightly more than in pure graphite. Crystallite thickness is reported as 1.2 nm by Heywood [23] and 1.4 nm by Ishiguro [27]. There are two to five platelets of hexagonal face-centred arrays of carbon atoms per crystallite. Dislocations and five- and seven-membered rings produce surface wrinkling. Heat treatment above 1000°C induces crystallite growth and increasing order in the structure [28].

Otto et al. [29] found similar surface areas when using either argon or carbon dioxide as adsorbent. The surface areas of soots as measured by BET analysis using nitrogen at 77 K as adsorbent give results in the range from 20 [30] to 230 $m^2 g^{-1}$ [29]. Since the theoretical surface area of smooth spheres of diameter 25 nm and density 2000 kg m^{-3} is 120 $m^2 g^{-1}$, the extent of pore surface is not large. The data generally suggest that the pore surface area is less than 100 $m^2 g^{-1}$.

Ahlström and Odenbrand [19] found that the BET surface area of a diesel soot increased from about 35 to 270 $m^2 g^{-1}$ simply by heating to 600°C under nitrogen. This implies that the SOF present is plugging some already-existing micropores.

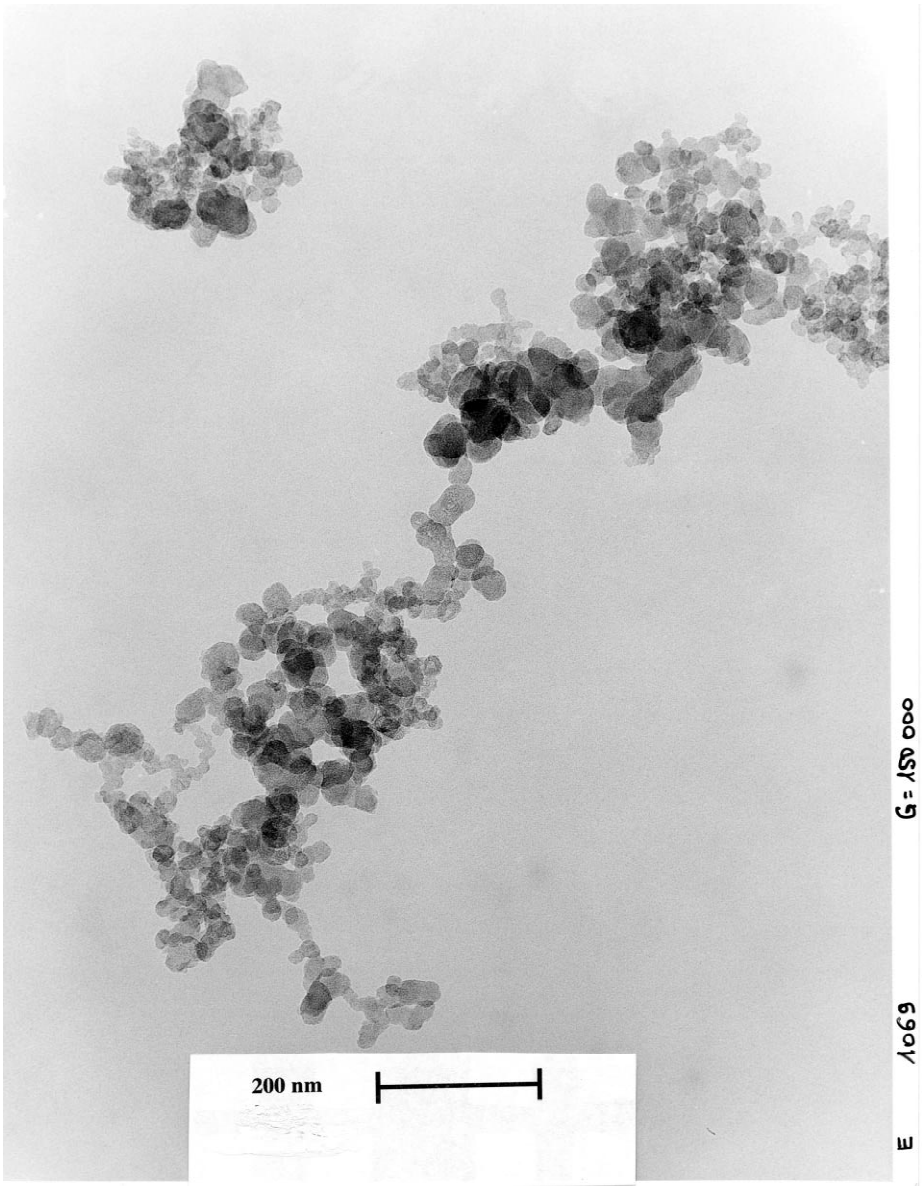

Fig. 1. Micrograph of diesel soot, showing particles consisting of clumps of spherules.

The sizes of the pores in spherules of some carbon blacks have been measured by Stoeckli et al. [31]. They have a slit shape typical of carbon and are of the order of 1 nm in width, compatible with the half-width of 0.4–0.5 nm measured by Buczek et al. [32] in activated carbon. The specific internal surface area (i.e. excluding the external surface) was 70–140 $m^2\ g^{-1}$ depending on the measurement technique. The void space in the spherules was between 0.04 and 0.075 $cm^3\ g^{-1}$, which indicates porosities in the range of 8–15%. Negligible SOF is present in carbon black.

The density σ_b of uncompacted beds of soot and carbon black ranges from 60 to 400 kg m^{-3}, which corresponds to a wide range of consolidation. Mechanical compaction of soot beds can increase the density to over 500 kg m^{-3} [33]. The porosity of the bed ϵ_b is given from the bed density σ_b and the spherule density σ_p by:

$$\epsilon_b = 1 - \frac{\sigma_b}{\sigma_p}$$

If the spherule density can be taken as 2000 kg m^{-3}, the equivalent porosities for the bed densities mentioned above are therefore 0.97–0.80. These porosities represent the

overall bed, and will be a combination of particle porosity and the void space in between. The intra-particle voidage of some carbon black particles was measured by Lahaye and Ehrburger-Dolle using thermoporometry [34]. They conclude that single particles of commercial carbon blacks are formed by strings which are a few (2–3) spherule diameters in thickness.

Many workers investigating diesel trap regeneration have substituted a commercial carbon black for diesel soot because it has very similar properties to the soot, and is generated in a controlled, reproducible manner [16,17]. The spherule size, surface area and overall reactivities tend to be very similar. However, some differences between the two in the progress of combustion can be identified [17].

4. Gasification

4.1. Gasification processes

Although the combustion of carbon is an ancient practice, scientific understanding of the phenomenon is still the subject of extensive research. The theory of the oxidation of a solid carbon by oxygen, steam, carbon dioxide or nitrogen dioxide involves both chemical kinetics with the consequent heat transfer, and mass transport at a number of levels. Gaseous oxidant must move to the surface and be adsorbed to form surface intermediates, which then rearrange, desorb and escape into the gas phase. The carbon surface may be the wall of a pore deep inside the solid, so that diffusion of oxidant from, and of product to, the bulk gas phase is also involved.

In order to systematise the discussion, combustion will be considered at low ($<$800°C) and high temperatures ($>$800°C). Low temperature conditions apply to many laboratory systems and to the regeneration of diesel traps where the material is present as a bed, i.e. aggregated. The high temperatures tend to apply to flame situations where entrainment flow applies, i.e. isolated particles are present.

When oxidation rates are specified on a surface basis it is usual to consider three regimes (see for example Smith [36]). Regime I applies when the oxidant fully penetrates the solid and all the internal surface is reacting, regime II when oxidant penetration is partial and diffusion into the particle is insufficient to supply all the reaction, and regime III when reaction takes place at the outer surface only.

Fundamental to the analysis of the combustion of porous solids is the effectiveness approach pioneered by Thiele. It will be applied here both to reaction within an individual spherule and to the whole of a soot bed. When applied to porous spherical particles with the reaction in oxidant taken as first order, the Thiele modulus θ [37] is:

$$\theta = \frac{d}{2}\left(\frac{\sigma_p k \beta}{D_e \sigma_{ox}}\right)^{\frac{1}{2}}$$

where d is the particle diameter (m), σ_p is its density (kg m^{-3}), k is the carbon reaction rate (kg kg^{-1} s^{-1}), β is the stoichiometric mass ratio of oxidant to carbon, D_e is the effective diffusion coefficient (m^2 s^{-1}) and σ_{ox} is the bulk gas concentration of oxidant (kg m^{-3}). The modulus is applied by means of the effectiveness factor which represents the fraction of internal surface which is able to react as if it were exposed to the surface concentration of reactant gas [37].

When the Thiele modulus is large ($\theta > 1$), the reaction rate outstrips the ability of diffusion to supply reactant and the effectiveness factor is small. When θ is small, diffusion dominates reaction and the effectiveness is high. Such factors as particle size, pore structure and particle temperature determine the combustion mode. For carbon oxidation, the coefficient β depends on the primary product of oxidation, being $4/3$ when carbon monoxide is the product and $8/3$ for carbon dioxide.

Because the nature of the combustion is strongly influenced by the penetration of oxygen into soot structures, the evaluation of diffusion within the material becomes of fundamental importance. This applies to diffusion both within an individual spherule and within a bed of particles. Both of these aspects are discussed below (Sections 5.1.2. and 5.1.3.).

4.2. Experimental equipment

Because of the experimental similarities, the same equipment is used for all four oxidants, O_2, CO_2, H_2O and NO_2.

4.2.1. Low temperature oxidation

The low temperature ($<$800°C) oxidation properties of soot which are of interest are the intrinsic kinetic rates, the ignition behaviour and the spread of an oxidation front through a bed. Most of this work is driven by the need to understand the regeneration characteristics of particulates in regenerative traps attached to diesel exhausts [21]. In doing so, it is important to identify the gasification behaviour of carbon both from the individual spherules, and from the bed as a whole.

Much effort has been expended in studying low temperature soot oxidation, under catalysed and uncatalysed conditions. Because of the slow reaction rates at low temperatures, all these studies were carried out on soot beds. To obtain accurate kinetics, the beds may be diluted with a large excess of inerts such as quartz [38], kaolin [39], silicon carbide [17] or aluminium oxide, with or without catalyst [15]. This diminishes the temperature rise which results from reaction and facilitates the transfer of oxidant within the bed.

Both pseudo steady-state and transient experiments have been carried out. The equipment used at low temperatures is generally a thermogravimetric analyser or a fixed bed. Some specialised equipment has been developed to simu-

late diesel soot deposits in exhaust filters (see Section 4.2.1.3.).

4.2.1.1. Fixed beds. The beds are kept comparatively thin and therefore operate in differential mode with negligible change in concentration of oxidant, except in some cases for the exceptionally reactive NO_2. For kinetic measurements, the systems are generally run isothermally, with an inert gas passing through the system during heatup until the desired combustion temperature is reached. A complementary mode is temperature programmed oxidation (TPO), in which the sample temperature is raised slowly under oxidising conditions and the gases evolved are continuously analysed. This approach is useful in identifying reaction mechanisms and the temperatures at which they occur.

The carbon beds studied by Neeft et al. [17] were diluted 10:1 by mass with silicon carbide. A commercial carbon black Printex U and a diesel soot were used. Ciambelli et al. [39] used a 100:1 excess of quartz beads to dilute the sample. Ahlström and Odenbrand [19] did not dilute the bed of uncatalysed soot but used a small fixed bed at the high space velocity of 70 000 h^{-1}, which should be sufficient both to control temperature and to ensure an adequate oxygen supply.

Ma et al. [40] promoted oxidation by irradiating a heated bed with microwaves. Diesel soot was found to respond better than a commercial carbon black.

4.2.1.2. Thermogravimetric analysis. There have been a multitude of studies, some with temperature ramping and others isothermal. Ramping tests are useful for identifying the quantity of adsorbed material (SOF) and the temperature of initiation (see Section 5.1.1.3.). Fig. 3 is typical of the thermograms obtained. The loss of SOF appears as the initial decline in mass. The burnoff of catalysed soot begins at a lower temperature than uncatalysed. TPO can be readily carried out in a thermobalance, but isothermal tests are better for measuring kinetic rates.

There is a range of thermobalances on the market, with various configurations of sample containment/gas flow contact configurations. If care is taken to ensure that the temperatures recorded are those of the sample, reliable reaction rates can be obtained for particles in the pulverised fuel size range [41]. A new design of thermobalance permits flow-through operation of the reactant gas, which should minimise mass transfer limitations.

However, this may not be the case with soot burned in a crucible. Though the effectiveness factor may indicate regime I combustion within the bed, transport limitations can apply between the mouth of the crucible and the bed surface. In a series of DTG studies, Gilot and co-workers [42–45] studied the interaction between kinetics and mass transfer. The transport of oxygen to the surface of a sample in a DTG crucible is by diffusion. Because of the large surface area of carbon per unit volume of sample and poor diffusion rates, the available oxygen then is rapidly removed by reaction. This results in combustion being limited to the surface of the bed, with the active layer being less than 1 mm in thickness [43].

Reported rates which do not take account of these effects may be too low [44]. This will especially be true at the higher temperature range of a test series. Even if a soot sample is diluted with an inert solid, the supply of oxygen can be limited. These aspects are developed later in Section 5.1.3. concerning burning in a bed.

4.2.1.3. Other systems. A simple fused silica flow reactor containing 150 mg of soot in a stainless steel pan was developed by Murphy et al. [46] to measure ignition temperature. The temperature of the reactor was slowly raised in a furnace and ignition was determined by a rapid rise in bed temperature as measured by a thermocouple.

Purpose-built equipment has been developed to identify ignition behaviour under realistic diesel trap conditions. In each case a circular soot bed was formed on a porous ceramic substrate and simulated exhaust gases were passed through it. In the apparatus of Herz and Sinkovitch [47] the sample was irradiated with an IR heating lamp through a calcium fluoride window. An IR pyrometer and a video camera recorded the surface temperature and the condition of the bed.

This type of apparatus was copied [48] and designated an RVVR (reactor to visualise and video regeneration). The ignition behaviour in this version was found to be similar to that found by Herz and Sinkovitch [47] (see Section 5.1.1.3.). Various bed masses, thicknesses, heating regimes and oxygen concentrations were trialled.

The beds used by Petersen [49] were collected on a filter substrate directly from the exhaust of an operating engine. The substrate was transferred to a flow reactor where it was ignited by preheated gas. Three thermocouples measured bed temperature across a radius.

There are many studies reported for operating engines with in situ regeneration, mostly for catalysed systems (Section 5.2.). Since they provide little fundamental data, they will not be described here.

4.2.2. High temperature oxidation

High temperature combustion takes place inherently in flames after the formation of soot. For instance, it is estimated that more than 90% of the soot formed in diesel engines is combusted before the exhaust gases leave the cylinder [23].

4.2.2.1. Laminar burners. Studies at flame temperatures have been carried out in laminar flow burners [25,50,51], generally directly coupled to a sub-stoichiometric soot-generating burner. The system used by Lee et al. [50] incorporated both steps into the one burner by forming an annular column of soot conveyed by a vertical gas flow

which was attacked by oxygen supplied around the periphery of the column.

In the investigation of Neoh et al. [25] freshly formed soot was burned in entrainment flow at temperatures of 1580–1860 K, using light scattering and absorption techniques to measure particle number populations and size. A flat flame secondary burner was fed with the products of a substoichiometric primary flame burning the fuel.

4.2.2.2. Shock tubes. The high temperatures produced by the compression wave in a shock tube have traditionally been used to investigate gas phase reactions over very short time intervals. Soot can also be studied, because the small spherule size (high surface area) allows significant burning to occur during the milliseconds of elevated temperature [52,53]. The soot is suspended in the gas near the reflecting wall before the shock is initiated. It is claimed that the shock assists in dispersing any aggregates [52]. Temperature is calculated from the initial gas conditions and wave velocity; temperatures up to 3500 K have been achieved.

Roth et al. [53] burned soot in suspension using a shock tube to initiate combustion. They measured CO/CO_2 concentrations using IR-diode laser and the particle properties with in situ laser light extinction.

5. Gasification with oxygen (combustion)

5.1. Non-catalytic combustion

The oxidation of carbon is catalysed by a range of metals, which can introduce different oxidation pathways. For this reason catalytic activity will be reviewed under a separate heading.

5.1.1. The chemistry of carbon oxidation

Detailed investigations of carbon oxidation show that molecular O_2 and the O and OH radicals all participate in soot oxidation [54]. OH is particularly effective [50,53]. Roth et al. [55] showed that hydrogen peroxide will assist soot oxidation at low temperatures, due to the presence of high concentrations of OH radical. The activation energy is very low with this reagent, namely 11 kJ mol^{-1}.

During oxidation at 500°C Ishiguro [27] found that the IR spectra showed increased C=C stretching vibration with increasing burnout, indicative of the presence of polycyclic compounds. At the same time the intensity of the C=O peak decreased.

Ismail and Walker [56] found that there are 'superactive' sites in Saran char which generate measurable reactivity to oxygen at temperatures around 200°C. The downwards extrapolation of higher temperature results predicts that no reactivity should exist. The sites are rapidly destroyed at higher temperatures.

As a result of low temperature (150–450°C) O_2 adsorption/desorption experiments on a lignite char and Spherocarb, Lear et al. [57] postulate the formation of a metastable oxide to explain the initial increase in weight. The metastable complex involves dioxygen which after adsorption desorbs only after a time delay or at higher temperatures, giving CO as the dominant product.

A good introduction to carbon oxidation is provided by Marsh [58]. Moulijn and Kapteijn [59] argue that at gasification temperatures the carbon surface will be relatively simple. They identify three types of carbon–oxygen complex of increasing stability: carbonyl, semiquinone and pyrone groups. Only a fraction of the oxygen-containing complexes take part in gasification reactions [60].

Ahmed et al. [61] examined thin films of pyrolytic carbon deposited from a sub-stoichiometric methane flame. From temperature-programmed desorption (TPD) they identified two types of adsorbed oxygen complex, and propose different sites for CO and CO_2 release.

Du and co-workers [62,63] examined the adsorption/oxidation steps of oxygen with a soot produced in a laboratory premixed ethylene flame. This method of preparation ensured that no metals were included. The mean spherule size was 43 nm. By TPD they identified a critical activation energy for desorption, below which the oxygen complex is rapidly desorbed and above which it is persistent. This critical value varies exponentially with temperature but only slightly with time.

Du and co-workers [62,63] tested the hypothesis of Ahmed [61] and others that two types of adsorbate are present. They found a range of activation energies with two maxima, rather than two distinct activation energies corresponding to desorption at each site. The activation energies do not change with extent of burnout. The desorption energy for the step which releases CO was 285 and 335 kJ mol^{-1} for CO_2.

The more active sites filled (forming CO) during the adsorption phase and only the slower (CO_2) sites were active during oxidation. The activation energy during oxidation was approximately 145 kJ mol^{-1}. The occurrence of adjacent active sites with surface migration and a Gaussian range of activation energies was incorporated into an extensive model of the system by Du and co-workers [62,63] which predicts most of their experimental data.

The action of the oxidants O_2, H_2O, CO_2, NO, N_2O and NO_2 involve at least two steps: (i) an O-atom is transferred from the gas to form a solid complex, and (ii) the complex decomposes and a C-atom is lost from the surface. The two-step sequence involves oxidant at each step and produces carbon monoxide. The dominant parameter is oxygen occupancy, which is a function of the oxidant. Molecular oxygen O_2 produces a heavily occupied and hence reactive surface at low temperatures.

The reaction scheme proposed by Marsh and Kuo [58] involves free carbon sites C_f, chemisorbed localised molecular oxygen $C(O_2)$, chemisorbed mobile molecular

oxygen $C(O_2)_m$, chemisorbed localised atoms of oxygen C(O) and chemisorbed mobile atoms of oxygen $C(O)_m$:

$$C_f + O_2 \rightarrow C(O_2) \text{ or } C(O_2)_m$$

$$C(O_2)_m \rightarrow C(O) + C(O)_m \text{ or/and} \rightarrow C(O)_m + C(O)_m$$

$$\text{or/and} \rightarrow C(O) + C(O)$$

$$C(O) \rightarrow CO$$

$$C(O)_m \rightarrow CO$$

$$C(O)_m + C(O)_m \rightarrow C_f + CO_2$$

$$C(O)_m + C(O) \rightarrow C_f + CO_2$$

$$CO + C(O) \rightarrow C_f + CO_2$$

$$CO + C(O)_m \rightarrow C_f + CO_2$$

$$O_2 + 2C(O) \rightarrow 2CO_2$$

Transient operation of a fixed bed at temperatures between 350 and 700°C was carried out by de Soete [38] to identify gasification mechanisms. A bed of soot diluted with quartz beads was brought to pseudo steady-state conditions under a flow of oxidant, and then the gas flow was switched to nitrogen. This permitted the rate constants for the overall gasification, oxidiser adsorption, CO desorption and CO_2 desorption reactions to be determined. The oxidants used were oxygen, steam and carbon dioxide.

The apparent combustion rates of soots generated from pure hydrocarbons, namely an aromatic (α-methylnaphthalene, α-MN), and an aliphatic (*n*-hexadecane, *n*-HD) were measured by this technique. Fig. 2 shows the relative magnitudes of the kinetic rates of the O_2 adsorption (k_1 P_{O_2} for 21 kPa partial pressure), CO desorption (k_2) and CO_2 desorption (k_3) reactions as defined by de Soete [38]. The rate of adsorption of the oxidiser k_1 P_{O_2} is lower than the desorption steps in this temperature range, especially as the surface coverage is low. Adsorption completely controls the reaction processes and the adsorption kinetics are always close to the overall carbon gasification rate. The coverage of active sites was low, and the reaction order was virtually 1.0. The ratio of CO to CO_2 in the offgas rose with temperature, but was generally of the order of unity.

Most experimental studies of soot combustion are carried out with the SOF still in place, and its presence could influence combustion behaviour. De Soete [38] found a difference in the kinetics of soot with SOF present and with it removed by treatment with nitrogen at 1100°C. The thermally-treated α-MN and *n*-HD materials (called char) showed a diminished reactivity at temperatures below about 600°C (900 K), but similar behaviour above this temperature.

There is little indication that the adsorbed hydrocarbons facilitate ignition during slow heatup tests [49,64]. They tend to be vaporised and therefore lost as the solids are brought up to ignition temperature. Distinct conversion peaks for SOF and carbon are common in TPO outputs, e.g. Querini et al. [65].

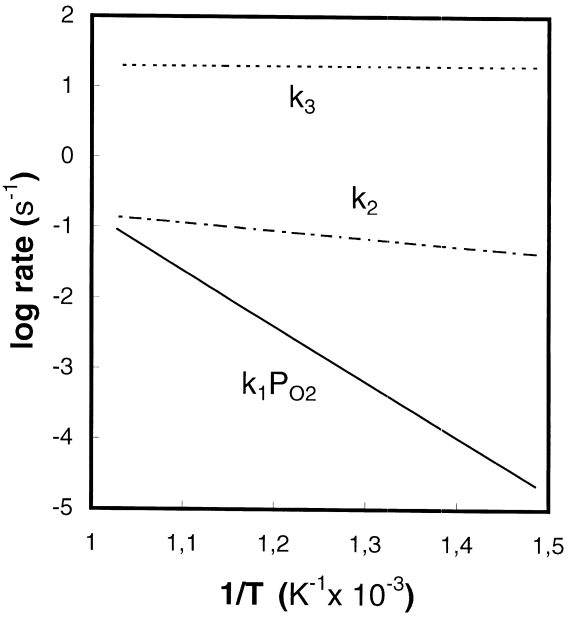

Fig. 2. Influence of temperature on the rates of adsorption of oxygen and desorption of oxidation products from a soot surface [38]; k_1 P_{O_2} = adsorption of oxygen, k_2 = desorption of CO, k_3 = desorption of CO_2.

Ishiguro et al. [27] found that the size of the layer planes of crystallites was 0.7–1.0 nm when unburned, but rose to 2–4 nm at 75% burnoff. At the same time the crystallite thickness increased to 1.6 nm. These authors report that the turbostratic outer layers become more crinkled as burnout proceeds, no doubt as a result of the expansion. They also identified small flakes of crystallite spalling of the outside layers and conclude that this is the result of strain energy in the layer plane.

A number of studies have shown that the initial stages of combustion display anomalously high combustion rates [17,38,39], which has been attributed to the removal of SOF. However it is generally accompanied by a rapid initial rise in pore area, which indicates that blocked pores are being opened up to adsorbent. It may involve chaotic edge carbons as well as SOF.

De Soete [38] found that oxygen adsorbates occupied only a small fraction (<5%) of the surface sites. This result was confirmed by Ma and Haynes [66] for spherocarb oxidation at low temperatures. They conclude that the carbon surface displays heterogeneity with regard to adsorption processes. The adsorption step results in the release of a molecule of CO or CO_2 for every molecule of O_2 adsorbed:

$$-C + O_2 \rightarrow -C(O) + CO, CO_2$$

5.1.1.1. Primary products. The ratio of carbon monoxide to dioxide in the product gases is dependent on the supply of oxygen, e.g. the concentration in the gas [15]. With an excess of oxygen at low temperatures, the ratio CO/CO_2 has been reported as <0.12 [67], but mostly is of the order of unity [16,17,38,42]. At temperatures up to 600°C, it rises with temperature, but falls with the addition of water vapour as a result of the water gas shift reaction [17]. Ahlström and Odenbrand [19] showed that in the presence of water vapour, the selectivity for the production of CO is dictated by the water gas shift equilibrium.

At higher temperatures, CO is the dominant primary product. However, above 700°C, CO begins to be homogeneously oxidised to CO_2 and conversion is virtually complete at 800°C [16].

5.1.1.2. Order of reaction. Order of reaction has traditionally been expressed as an exponent on the reaction gas partial pressure P_{ox} or concentration:

$$k = A \exp\left(-\frac{E}{RT}\right) P_{ox}^{n} \quad s^{-1}$$

However, the values for n fitted to experimental results have varied widely and have been difficult to interpret. The bulk of the studies at low temperature report the order of reaction in oxygen to be unity [16,29,33,38,42]. De Soete [38] found that adsorption of oxygen controlled the rate (see Fig. 2), which implies a first order system.

Following Essenhigh [68] for the case where there is no boundary layer resistance to mass transfer, we can write the rate in terms of the adsorption and desorption steps:

$$\frac{1}{k} = \frac{1}{k_a P_{ox}} + \frac{1}{k_d} \quad s$$

If the desorption rate as given by k_d is much greater than the adsorption rate term $k_a P_{ox}$ as was found by de Soete [38], then $k \propto P_{ox}$, i.e. the reaction is first order. In contrast, Neeft et al. [17] found orders of 0.76–0.94 at temperatures around 500°C, depending on burnout, and Petersen found 0.5 at the same temperature [49]. Ciambelli et al. [69] consistently found n to be 0.8 for carbon black burned at 593 K.

The experimental order of reaction found by Du et al. [63] was 0.77 for CO release and 1.0 for CO_2 release. The combination of these two reactions reactions gives an overall order of reaction around 0.83 in the temperature range 750–850 K. The CO/CO_2 ratio was near unity, in keeping with other results.

The empirical approach to reaction order represented by the above expression has been criticised by Essenhigh [68], who insists that a theoretically-based expression such as a Langmuir isotherm should be employed. He also produced the extended resistance equation or ERE to describe the progress of solid particle combustion. From fundamental principles it can be shown that changes in density and particle diameter during burnout are related by:

$$\frac{\sigma}{\sigma_o} = \left(\frac{d}{d_o}\right)^{\alpha}$$

where the subscript o denotes initial conditions before combustion. As a guide, α is zero for a true shrinking core situation, of the order of 1–6 for regime II conditions and greater than 6 for regime I.

It follows from consideration of the ERE that reaction order is a function of temperature [70]. Essenhigh's analysis [68] for pulverised particles (~100 μm) in experiments gives the effective reaction order as zero at 1000 K, rising to unity at 2000 K. This implies that the desorption rate k_d controls at low temperatures, but the adsorption rate at high temperatures, which is contrary to the findings of de Soete. As will be seen later, some aspects of Essenhigh's analysis may not apply to soot spherules.

At high temperatures, the reaction order is reported as unity by Lee et al. [50]. The correlation of Nagle and Strickland-Constable [71] is first order at low oxygen partial pressures, but approaches zero order at higher pressures. Park and Appleton confirmed this trend at oxygen pressures greater than one atmosphere [52]. For air at temperatures below 1500 K, the value is practically 1.0. Roth et al. [53] found the system was roughly first order with respect to O_2 in the range 1600–2500 K.

5.1.1.3. Initiation and ignition. The processes of ignition are defined differently by different authors and for different equipment. In DTG temperature ramping tests, initiation is defined as the temperature at which the mass loss trace under an oxidant flow first deviates from that under an inert gas. Fig. 3 depicts such a test with the initiation temperature marked T_{in} [64]. Lahaye et al. [15] use the term acceleration temperature (or onset of effective oxidation) to describe the intercept on the temperature axis of the linear part of the burning curve (weight loss v. temperature). The term ignition in a DTG is generally used to indicate a temperature runaway.

Similarly, ignition in a fixed bed test signifies a thermal runaway, with a sharp peak in temperature and rapid consumption of the bed [64]. Generally ignition occurs locally and then spreads rapidly through the bed.

In an RVVR, ignition temperature is that at which the irradiated part of the bed sustains a rapid temperature rise and begins to glow [47,48]. Herz and Sinkevitch [47] and McCabe and Sinkevitch [72] found that ignition was indicated by a sharp, easily discernible spike in the temperature. The progress of burning subsequent to ignition was erratic, showing snake-like patterns which left large areas unburned. The ignition temperature T_i was sensitive to the oxygen content of the gas, but only slightly to its velocity, provided that it exceeded 1 cm s^{-1}. Metals added to catalyse the combustion lowered T_i substantially.

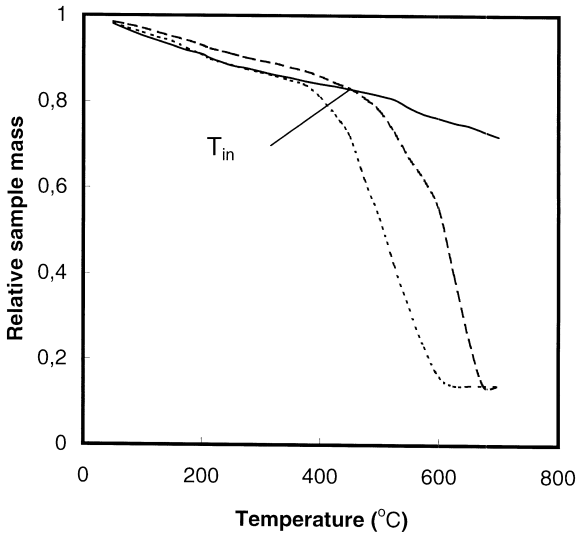

Fig. 3. DTG thermograms of diesel soot [64]: (—) under nitrogen, (- - -) under 10% oxygen uncatalysed, (· · ·) under 10% oxygen catalysed with cerium.

A mathematical model of the RVVR system was developed by McCabe and Sinkevitch [72], based on a heat balance over the soot layer. The input term is the heat of reaction and the output is only the convective transport to the gas. The bed soot is assumed isothermal and the sensible heat of the gas phase is assumed to be negligible, compared to the solid. The model gives an adequate description of the ignition phenomena. An extension of this model using measured kinetics for catalysed and uncatalysed soot successfully predicted the differences in their ignition temperatures [64].

Lahaye et al. [15] found constant surface area on burnout, ascribed to layer combustion. Above 600°C they also found what was termed 'autoignition', where the initial reaction rate showed an almost instantaneous step before proceeding at a more controlled rate.

Application of the Semenov analysis to soot ignition allows values of comparative ignition temperatures to be derived. Following Lahaye [15], for equilibrium at the ignition point:

$$mC\frac{\mathrm{d}T_{\mathrm{i}}}{\mathrm{d}t} = Q_{+} - Q_{-} = 0 \text{ and } \frac{\mathrm{d}Q_{+}}{\mathrm{d}T_{\mathrm{i}}} > \frac{\mathrm{d}Q_{-}}{\mathrm{d}T_{\mathrm{i}}}$$

where m, C and T_{i} are the mass, specific heat and ignition temperature of the solid, respectively, and $Q_{+,-}$ are the heat production and loss rates. Under the same test conditions the loss by heat transfer will be of the same form so that two different soots with different activation energies $E_{1,2}$ and pre-exponential factors $A_{1,2}$ will be related by:

$$\frac{E_1 A_1 T_{\mathrm{i2}}^2}{E_2 A_2 T_{\mathrm{i1}}^2} \exp\left(\frac{E_1 T_{\mathrm{i2}} + E_2 T_{\mathrm{i1}}}{R T_{\mathrm{i1}} T_{\mathrm{i2}}}\right) > 1$$

where $T_{\mathrm{i1,2}}$ are their ignition temperatures. The experimentally measured and calculated ignition temperatures in the DTG were found to be in satisfactory agreement.

5.1.1.4. Reaction kinetics. Low temperature activation energy is found to cover a range, namely between 102 and 210 kJ mol^{-1} [15,17,19,38,73]. The low value of 102 kJ mol^{-1} was ascribed to the presence of a high concentration of metals in the sample [19], which could have acted as catalysts. Values between 140 and 170 kJ mol^{-1} appear frequently. A value of 142 kJ mol^{-1} was found by Otto et al. [29] with 10 mg of undiluted soot in a DTG, but in view of the effect of diffusion described by Marcucilli et al. [16], this figure is probably low.

De Soete [38] found that the oxidation rate of soot from an aromatic source was higher than from an aliphatic. In both cases there were changes in activation energy at moderate temperatures, around 800 K (Fig. 4). Since the activation energy increased at the higher temperatures, this cannot be interpreted as a movement from regime I to regime II combustion.

Fig. 4 plots reaction rates based on carbon consumption from a number of investigators, normalised to 10 kPa partial pressure of oxygen. The rate constant k (s^{-1}) based

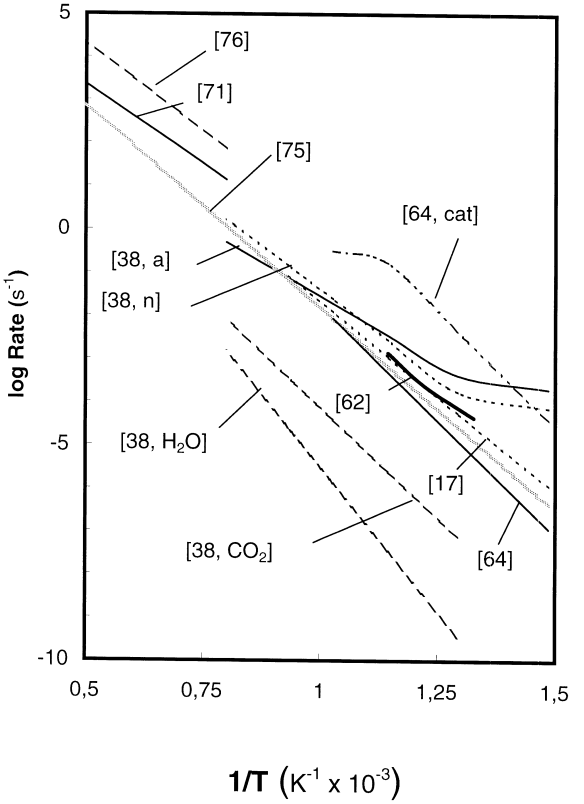

Fig. 4. Arrhenius plot of some kinetic rates of soot gasification using oxygen, steam and carbon dioxide as reactant.

on carbon removal is related to that based on oxygen consumption K (s^{-1}) by:

$$K = \frac{\beta \sigma_b}{\sigma_{ox}} k \quad s^{-1}$$

where σ_{ox} is the density of oxygen in the gas phase. Care is required in the definition of reactivity in the Thiele modulus, which may be in terms of k as noted in Section 4.1. or in terms of K (Section 5.1.3.).

There is good agreement between the different authors who used a number of different techniques, and with other results not shown [74]. The low temperature data of de Soete [38] deviate from the other sets. Note however that all these rates will be influenced by the combustion mode and the subsequent formation of additional surface area.

Also shown on Fig. 4 is the generalised correlation for carbon oxidation deduced by Smith [75] for a wide range of materials and oxidation conditions, corrected to 10 kPa oxygen and 120 $m^2\ g^{-1}$ surface area of carbon. It falls in the middle of all the data, so that in the absence of other information, it can be used to estimate the combustion rate of uncatalysed soot.

The semi-empirical relationship of Nagle and Strickland-Constable [71] is most-commonly introduced to describe high temperature combustion. Two types of active site are proposed: a more reactive type A site and a less reactive B. Thermal rearrangement of type A sites into B takes place according to:

$$x = \left(1 + \frac{k_T}{P_{O_2} k_B}\right)^{-1}$$

where x is the fraction occupied by type A sites and K_T and k_B are rate constants. The rate equation is:

$$r = 120 \left[\left(\frac{k_A P_{O_2}}{1 + k_Z P_{O_2}} \right) x + k_B P_{O_2} (1 - x) \right] \quad kg\ m^{-2}\ s^{-1}$$

where k_A and k_Z are further rate constants. At temperatures below 1700 K, the value of x is ~1 and the activation energy is effectively 143 kJ mol^{-1}.

The Nagle/Strickland-Constable approach was tested extensively by Park and Appleton [52]. They found it to accurately describe the high temperature behaviour, but to somewhat underestimate the rates. Similar reservations about the rates have been expressed by other authors [51,76].

For high temperatures, an expression by Lee et al. [50] and a more recent one from Leung et al. [76] are also available. The correlations of Nagle and Strickland-Constable and Leung et al. [76] for higher temperatures are also shown on Fig. 4, assuming a surface area of 120 $m^2\ g^{-1}$. The results are not in good agreement and both are higher than the correlation of Smith [75]. They are however in the vicinity of an extrapolation of some of the low temperature data.

5.1.2. Analysis of burning data for spherules

At all size scales, it is necessary to take account of mass transfer effects. This applies to individual spherules as well as to assemblages of soot particles in beds.

There is uncertainty as to the mode of burnout of the individual soot spherules. In view of the elongated structure of aggregated soot particles, it is difficult to isolate the behaviour of individual spherules. They consist of densely packed carbon crystallites with a low porosity, which implies that the diffusion rate of oxidant into the interior would be low. It could therefore be anticipated that oxygen penetration is restricted, and that regime II or III conditions would apply.

In order to calculate the Thiele modulus it is necessary to know the pore dimensions. With the 1-nm pores estimated earlier, full penetration of oxidant is predicted at all temperatures below 1000°C. This comes about because of the short diffusion path (~10 nm), which more than compensates for any diminution of the diffusion coefficient in the narrow pores. Thus, regime I burning, rather than regime II or III is predicted.

The participation of micropores (<2 nm) in gasification reactions has been called into question on a number of occasions, for example Gavalas [77], Radovic [78]. Aarna and Suuberg [79] present evidence that this is in fact the case for a coal char. Since the pores in soot spherules are undoubtedly in the micropore range, there is justification for suggesting that the spherules will burn in a regime III mode.

Experimental resolution of this uncertainty has been difficult. Ishiguro et al. [27] report that an early investigation into the combustion of carbon black found that the centres of the spherules were preferentially burned and became void. The only recent work to confirm this result is by Gilot et al. [42], who studied Regal 600 carbon black at 60% burnout. Lahaye et al. [15] report 'channeling', i.e. internal slices of carbon were removed from spherules containing 3% cerium which were burned under kinetic control.

Based on their experimental results on burning in air, Neeft et al. [17] and de Soete [38] conclude that a shrinking core situation applies. De Soete offers no explanation for this conclusion. Neeft et al. base their statement on the reaction order for carbon as given by the relation for isothermal reaction:

$$\text{rate} = \text{constant}(1 - u)^m k \quad g\ g^{-1}\ s^{-1}$$

where u is the burnout and k is the reaction rate (s^{-1}). The value of m varied between 0.65 and 0.8 for the carbon black Printex U, but was difficult to fit for diesel soot. Because the shrinking core model requires that m be 2/3, the conclusion was drawn that shrinking core behaviour applies.

However, when one examines the rate versus time and rate versus conversion (burnout) curves for Printex U

presented by Neeft et al. [80], the former is 'exponential-like' and the latter is almost linear from $u=0.2$–0.9. Thus, the rate of reaction is almost directly proportional to the mass of carbon remaining. This is consistent with extensive oxygen penetration into the spherule, leading to decreasing density, i.e. regime I conditions.

A good set of data on the change in soot properties during reaction was collected by Ishiguro et al. [27] who oxidised samples of diesel soot at 500°C to 25, 50 and 75% burnout. They examined the products by electron microscope and reported the mean diameters of 2000 spherules at each burnout. Their results are internally consistent and the following relations for diameter and density in terms of burnout can be fitted to their data with good accuracy:

$$\frac{d}{d_o}=(1-u)^{1/6} \text{ and } \frac{\sigma}{\sigma_o}=(1-u)^{1/2}$$

From this data, the value of α in the ERE of Essenhigh is 3, which is typical of combustion in regime II, close to regime I conditions. A value <1 would be required for the shrinking core situation to apply. The second effectiveness factor η as defined by Essenhigh [70] is the ratio of the burning rate to the external burning rate. Since $\eta=1+3\alpha$, under the conditions used by Ishiguro et al. [27] the total rate of carbon removal is 10 times that on the exterior surface; an interior:exterior ratio of 9:1.

When applied to coal particles, the analysis of Essenhigh [70] predicts that the initial particle density is an important variable in determining the value of α. Dense particles of initial density $\rho_{po}\sim$2000 kg m^{-3} should burn in regime I ($\alpha=0$) and those with low initial density should have a higher value of α (~3). The very small diameter of the soot particles appears to invalidate this aspect of the analysis, as the Thiele modulus is always much less than unity.

The changes in surface area brought about by mass removal during gasification have been extensively studied. Generally, there is a diminishing rate of increase as combustion proceeds, with the value continuing to rise up to 50% burnout [16,27,29,49]. At higher burnoffs, the value may remain roughly constant [27,29], or fall [49].

The change in area depends on the gasification medium and the temperature. Gilot et al. [42] and Marcucilli et al. [16] found that the increase in area was greater during burning in air at 600 and 700°C than at 800°C (Fig. 5). This is consistent with there being greater penetration of oxygen (a higher effectiveness factor) at the lower temperature due to slower consumption by reaction. By extrapolation of these data, the original effective area can be considered to be 160 m^2 g^{-1}, rather than the 100 m^2 g^{-1} which was measured (see Section 3.). The increase predicted by burning under shrinking core conditions is also shown in Fig. 5, based on 160 m^2 g^{-1} initially. Burning approaches shrinking core conditions (regime III) at 800°C.

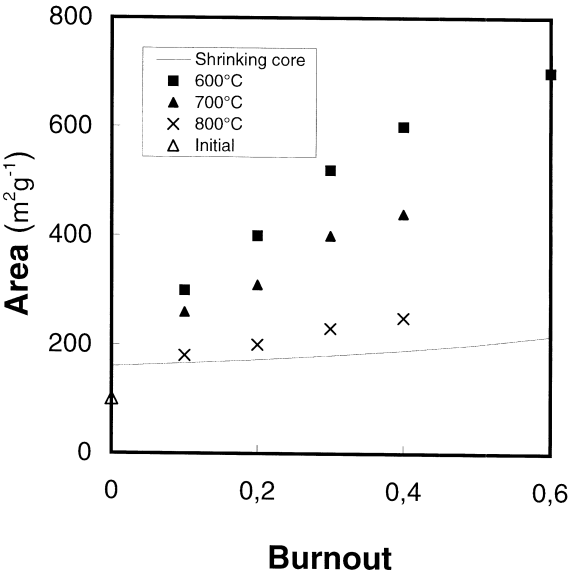

Fig. 5. BET surface area as a function of burnout with oxygen at different temperatures [42].

The same explanation for differences in BET surface area can be made when different gasification media are used. At the same extent of conversion, there are greater increases in area with gasification by steam and carbon dioxide at 400°C than with oxygen [29]. These less reactive oxidants should penetrate the spherules to a greater extent. It should be noted that the effectiveness factors calculated for all the conditions above were unity, but significant differences in area result.

At 50% burnoff under air, the increase in area is 60% for Petersen (480°C) [49], 100% for Otto et al. (450°C) [29] and Marcucilli et al. (600°C) [16], but 600% for Gilot et al. (600°C) [42]. These results are consistent with the behaviour of a highly purified carbon black (Graphon), which showed a 40% increase in area after 35% burnout [81]. If the change in spherule diameter follows the pattern found by Ishiguro et al. [27], the increase in theoretical outside surface on a mass basis should be 12% at 50% burnoff, simply as a result of particle shrinkage. In contrast Ishiguro et al. [27] found an increase in surface area of around 400% at 50% burnoff, but the initial value of 52 m^2 g^{-1} is less than the theoretical external area of 87 m^2 g^{-1} [25].

On balance, the experimental data suggest that significant oxygen penetration occurs at low temperatures.

Turning to high temperatures, the increased reactivity will decrease the extent of oxidant penetration. As reported above, Neoh et al. [25] believe that internal burning occurs, based mainly on theoretical considerations. For spherules, they predict an effectiveness of 0.74 for oxygen in 0.5-nm pores in 20-nm particles ($T=1775$ K). This suggests extensive penetration of oxidant.

They found a difference in behaviour between rich and lean flames. There was a rapid increase in the number concentration of particles in lean flames after about 80% burnout, which they attributed to fragmentation. It appears that the common material fusing the spherules into particles is removed, and the remains of the individual spherules are released.

In rich flames, the overall structure (chain) remains intact as the particle concentration remains unchanged. In both fuel-rich and lean flames the particle sizes decreased with burnout, rapidly in lean flames but only slightly in rich. The initial diameters were only about 80 nm, which the authors note is typical of the particle dimensions.

They explain the difference in terms of the reactivity of the OH radical compared to molecular oxygen. OH is a more active oxidant than O_2, and should produce less internal burning They estimated the effectiveness factors for pores of radius between 0.5 and 4 nm, the former to represent the pores inside a spherule, and the latter to represent inter-spherule gaps. They conclude that O_2 will penetrate the particles and disrupt them, while OH is unable to do this. Since OH is the main oxidant in rich flames, fragmentation is not observed in that case.

There are some difficulties with this interpretation of the data. The chains are long and the concept of size (diameter) is difficult to apply. The particles are small, isolated and of the same size as the mean free path of oxidant. The electron micrograph included in their paper shows that their structure is virtually linear (Section 3.), so that it is difficult to imagine there being any diffusion restrictions. The assumptions of the Thiele approach as applied to a particle do not appear to be relevant.

The differences in behaviour between lean and rich flames may be the result of differences in reactivity between OH and O_2, but this reactivity may relate to differences in carbon structure between the bulk material of the spherules and the interparticle deposits which bind the spherules together.

5.1.3. Analysis of burning data for soot in beds

The fixed bed systems mentioned above can be expected to give reliable kinetic data, provided that the convective gas flow is adequate to overcome mass transfer limitations, and the bed is diluted with inerts. However when one considers beds of soot contained in crucibles undergoing thermogravimetric analysis (DTG), mass transfer considerations must be addressed. Flows of oxidant gas are modest (perhaps 100 ml min^{-1}) and generally directed across the mouth of the crucible.

Neeft et al. [82] produced a model of heat and mass transfer between a crucible of soot and the surroundings. The mass transfer of oxygen is limited to that between the bulk gas and the sample surface. The oxygen concentration inside the bed is assumed to be uniform, which has been shown to be false [35]. However it satisfactorily explains thermal runaways during DTG analysis, but only in a qualitative manner. They emphasise, like Gilot et al. [83], that sample size should be limited.

The interaction between mass transfer and reaction in a DTG test is well illustrated by a series of papers by Gilot and co-workers [16,42–45]. Using samples of 5–40 mg, it was found that the absolute rate of mass loss (g s^{-1}) in isothermal tests was almost constant in each for most of the burnout (Note the rapid nearly-linear fall in mass in Fig. 3 for a temperature ramping situation). This suggests that a thin reaction zone was always present at the bed surface. The conclusion was supported by a unidimensional model of oxygen penetration into the bed, which demonstrated that diffusion was significant [43].

The effect of mass transfer in both the flow direction and normal to this was first demonstrated by means of a finite difference model of the gas space above the crucible and the bed within it [16]. In a typical DTG situation, convective mass transfer coefficients to the surface of the bed were found from:

$$h_m = \frac{\omega}{\sigma_g(y_o - y_s)} \quad (m\ s^{-1})$$

where ω is the surface mass flux of oxygen (kg m^{-2} s^{-1}), σ_g is the gas density (kg m^{-3}) and y_o and y_s are the bulk and bed surface mass fractions of oxygen. The values of h increase with temperature for the same flowrate, and also with sample mass because the bed surface was closer to the mouth of the crucible. The coefficients were of the order of 0.5 cm s^{-1}, which is capable of furnishing a surface mass flux of oxygen of perhaps 2×10^{-4} kg m^{-2} s^{-1}. Under the same conditions, molecular diffusion can supply approximately the same amount, which suggests that it is in fact the dominant mechanism.

That diffusion is supplying most of the oxygen to the bed surface in a DTG test was confirmed by modelling the space above the bed with computational fluid dynamics CFD [44,45]. The velocity vectors inside a crucible are virtually zero, even if it is a shallow crucible and facing the gas flow. The oxygen mass transfer contours are uniform and parallel to the bed surface.

Within the bed, diffusion is also the mechanism of oxygen transport. Although the beds have high porosities, the small dimensions of the component solids introduce significant diffusion constraints. Knudsen diffusion is therefore thought to operate. The Thiele modulus in the bed is high, so that the depth of penetration is shallow. This leads to surface layer burning as mentioned above.

A unidimensional model of the gas concentration within the bed was found to be adequate for the extraction of kinetic data from isothermal DTG tests [64]. The surface oxygen flux ω is known from the experimental rate of carbon loss, and the CFD model gives the mean surface mass fraction y_s. This can then used as a boundary condition for the unidimensional model. The expression for oxygen flux to the the bed surface in terms of

displacement from the surface x (m) in an isothermal bed of depth e (m) [43] is:

$$\omega = K\sigma_g \int_0^e y\,dx \quad \text{kg m}^{-2}\,\text{s}^{-1}$$

where K is the rate of consumption of oxygen (s^{-1}). The oxygen concentration at position x within the bed is:

$$y = \frac{y_s}{1+\exp(-2\theta)}\left[\exp(-2\theta)\exp\left(\sqrt{\frac{K}{D_e}}x\right) + \exp\left(-\sqrt{\frac{K}{D_e}}x\right)\right]$$

where $\theta = e\sqrt{(K/D_e)}$, the bed Thiele modulus. Then:

$$\frac{\omega}{\sigma_g y_s} = \sqrt{KD_e}\left[\frac{1-\exp(-2\theta)}{1+\exp(-2\theta)}\right]$$

Since K appears in θ, an iterative data fitting is required to evaluate it from the surface oxygen flux and concentration. With these techniques reliable kinetic data can be found, provided that appropriate values of D_e can be supplied.

Brilhac et al. [33] measured the effective diffusion coefficients of oxygen in soot beds of various porosities using a type of Wicke–Kallenbach diffusion cell. An experimental coefficient of 2.0×10^{-6} m^2 s^{-1} at $\epsilon = 0.82$ and 298 K is typical. The effect of porosity on the effective diffusion coefficient is shown in Fig. 6. Even a very open bed of low density results in a rapid fall in coefficient from the bulk value.

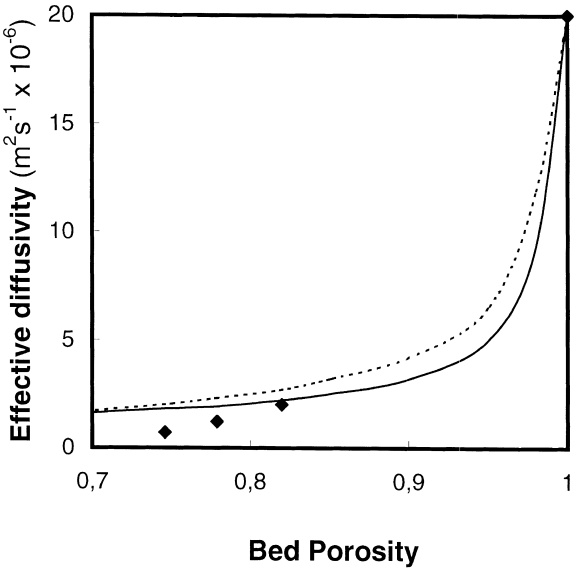

Fig. 6. The influence of bed porosity on the effective diffusion coefficient of oxygen in beds of carbon black — measured and predicted [33]: (-♦-) experimental; (- - -) Monte Carlo; (—) kinetic theory.

When estimating effective diffusion coefficients inside such beds, the usual random pore or 'swiss cheese' approach [84] is unsuitable. The aggregated structure of soot makes it an unusual carbon material, unlike chars, cokes and activated carbons, which can be regarded as solids with holes. Better results are obtained by regarding it as a collection of solid spheres with extremely high porosity, i.e. as a 'cannonball' or 'caviar' solid.

A simulation of the diffusion process based on the caviar model was developed by Brilhac et al. [33]. A Monte Carlo random walk approach to the passage of oxygen molecules through an array of randomly spaced spheres was used. This procedure tended to overestimate the measured effective diffusion coefficient, but was improved by considering the bed to be locally non-homogeneous (Fig. 6). A simpler kinetic theory model based on a mean free path and the mean kinetic velocity also produced acceptable results. In both cases, better estimates are produced if the local disposition of spherules is taken into account, that is, that both the particles and the void space in between are physically simulated.

5.2. Catalytic combustion

The pursuit of a technique for diesel soot control has prompted a plethora of research into the application of catalysts to lower ignition temperatures and so promote combustion [19,39,48]. For example, the ignition temperature of a soot in a thermobalance fell by 300 K in one case of catalyst addition [39].

Catalyst can be added either through the fuel, in which case it is incorporated into the soot spherules as they form, or physically mixed in after collection of the soot. The latter would correspond to the case of a soot filter whose surface is impregnated with catalyst via a wash coat. The auto industry favours the addition of catalyst to the fuel, as it ensures that the active components are intimately mixed with the carbon. Small concentrations of around 50 ppm are sufficient. However, most of the combustion studies reported in the literature use physically-mixed catalysis.

5.2.1. Catalyst-impregnated soot

A multitude of studies consist of empirical tests on operating engines fed with doped fuel [85–101] to list but a few. There are far fewer studies which focus exclusively on the oxidation of soot collected from flames or engines running on doped fuel [15,64,102,103]. The catalysts added to fuel take the form of soluble compounds (octanoates, naphthanates) of metals such as copper, iron, cerium, lead, manganese etc.

A comparison of the effect on reactivity of iron and copper additions to the fuel showed that copper produced a modest increase by a factor of around 5 at 600°C, and iron by a factor of 3 [102]. Although copper has been found to

be very efficient by all investigators, it is environmentally unacceptable [104]. Cerium has now emerged as the preferred fuel additive of automotive constructors and a system using it has been commercialised [105].

Lahaye et al. [15] produced soot by the pyrolysis of hydrocarbons, with and without cerium addition. The cerium is present as oxide [15]. Increasing cerium concentration diminishes the mean particle size of the soot during formation and lowers the ignition temperature under oxidation. Above 600°C very rapid oxidation (called autoignition by the authors) occurs. At low temperatures (<520°C), CO_2 is the only product but above this the ratio CO/CO_2 remains at about 0.5. The activation energy of combustion fell from 170 to 120 kJ mol^{-1} with the addition of cerium.

After running scores of tests on soots containing varying amounts of cerium oxide as obtained from engines operated under three different conditions, Stanmore et al. [64] found a significant ($\approx 10^2$) increase in reactivity with cerium present, but no change in activation energy from 210 kJ mol^{-1} (Fig. 4). Note the change in activation energy in their data above about 900 K, where reactivity no longer increases with temperature. This is similar to the auto-acceleration phenomenon described by Lahaye et al. [15], which has not been explained. Petersen [49] also found no change in activation energy with the addition of lead.

Some papers report only on the oxidation of SOF, which is composed mostly of lubricating oil [106,107]. In these tests the catalyst was impregnated with oil.

5.2.2. Physically-mixed catalyst

Turning to externally added catalyst, Murphy et al. [46] added metal chlorides dissolved in methanol to diesel soot and determined ignition temperatures. Copper was found to give superior performance compared to Mn and Co, lowering T_i by about 100 K.

Much attention has been focussed on the quality of contact between the carbonaceous material and the grains of a solid catalyst. This concept is developed particularly by Neeft and co-workers [80,108–110] and Ciambelli and co-workers [69,111–113]. If the catalyst grains are not in intimate contact with the carbon surface, their effect will be diminished. For modelling purposes, Ciambelli et al. [69] postulate two reactivity relationships, one for spherules within the field of action of the catalyst, and another for those initially outside.

Neeft et al. [80] developed two methods of mixing catalyst with soot, which they term 'loose' and 'tight'. The methods produced reproducible combustion behaviour, and permitted a more reliable classification of catalyst activity. The catalysts were prepared as particles of less than 125 μm size. In the loose mode, a 2:1 ratio of catalyst to carbon black was simply mixed together with a spatula. In the tight mode, a mixture at the same ratio was mechanically milled for an hour. In both cases the samples diluted with SiC were placed into a crucible and oxidation tests were carried out in a DTG/DSC. A wide range of metals was tested for catalytic properties [108,109], using a heating rate of 10 K min^{-1} in 21% oxygen.

As an example, the differences between the oxidation behaviours for the two contact systems using Fe_2O_3 and MoO_3 as catalysts are shown in Fig. 7. With tight contact, there is a considerable fall in the temperatures at which the reaction proceeded for both metals. However, MoO_3 is active in the loose condition but Fe_2O_3 is not. The activities of the catalysts were then assessed in terms of the 'combustion' temperature, i.e. the maximum temperature recorded in the DSC trace.

The action of catalysts can be determined from the form of the burnout trace [80]. Extremely active catalysts produce an initial increase in reaction rate with burnout up to $u>0.5$, followed by a decline. Less active catalysts show a declining or constant rate burnout. Neeft et al. [110] showed that if the monolithic trap in a diesel exhaust is coated with catalyst, the oxidation behaviour is similar to the loose contact condition. The full potential of a catalyst can be achieved only by the addition of a soluble

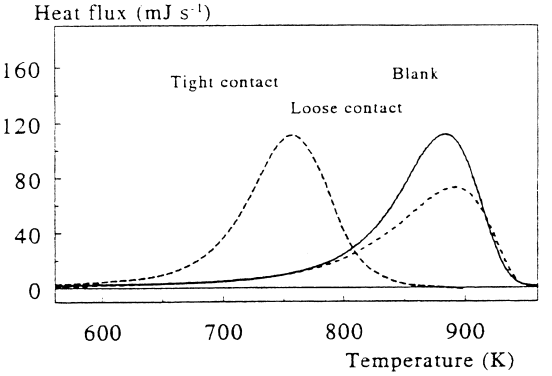

Tight versus loose contact mode Fe_2O_3 catalyzed soot oxidation.

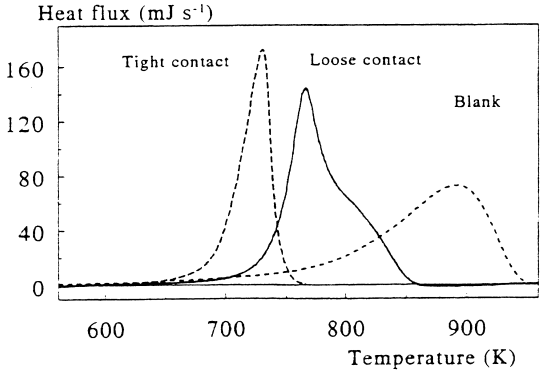

Tight versus loose contact mode MoO_3 catalyzed soot oxidation.

Fig. 7. Burning rates in a DTG/DSC of carbon black mixed with Fe_2O_3 and MoO_3 catalysts: loose and tight contact [109].

compound to the diesel fuel to ensure that it is incorporated into the soot spherules.

Of the straight metal oxides, PbO is the most active [80,114], but CuO and MnO_2 are also efficient. Courcot et al. [20] concluded that Cu^{2+} ions are the active sites with copper reagents. Copper is more active in the presence of chloride than other anions and Mul et al. [115] identify Cu_2OCl_2 as an oxidation intermediate.

The oxides of metals which readily change valency have been identified by Setzer et al. [116] as superior catalysts. Thus Cu, Fe and Co are far more active than Ni and Zn. Neeft et al. [109] found that the oxides Co_3O_4, V_2O_5, Fe_2O_3 La_2O_3, MnO_2 and NiO exhibit high to moderate activities in tight contact but hardly any activity in loose contact. Other oxides such as PbO, Cr_2O_3, MoO_3, CuO and Ag_2O are still active in loose mode, although at a reduced level. Neri et al. [67] found that Fe_2O_3 was a good catalyst for SOF oxidation but that CuO and V_2O_5 were better for the carbon component.

The catalysts tested by Ahlström et al. [117,118] were loaded onto γ-alumina which was used at a 10:1 mass dilution, while the reference (uncatalysed) tests were carried out with pure alumina. The arrangement must be considered as 'loose'. As a result, the gains in reactivity were modest, with V_2O_5 being best. It also resisted poisoning by the sulphur present in soot.

Ciambelli et al. [111] produced a version of tight contact by pounding the components together with a mortar and pestle. Like Neeft et al. [80], they found that the reaction rates were strongly influenced by the mass ratio of soot to catalyst R_m, finding significant falls in burnoff temperatures as R_m decreased.

Badini and co-workers [119,120] used a ratio of 1:1 soot to catalyst, which is probably too low to exercise good control of the thermal conditions.

When a mixture of soot and one of the following metal oxides is heated in the absence of gaseous oxidisers, CO and CO_2 are found as reaction products [38]. Good catalysts (CuO, MnO_2) produce CO_2 exclusively, while poor catalysts (CeO_2) produce both, and inactive oxides (Al_2O_3, SiO_2, La_2O_3) produce CO only in negligible quantities. This suggests an oxygen donor mechanism, rather than a mere electronic mechanism. The catalytic effect is due to the fact that carbon adsorbs metal-bound oxygen atoms (–MO) faster than molecular-bound oxygen.

Catalysed reaction mechanisms are evidently different from the uncatalysed condition — as the order of reaction, the activation energy and the primary products all change. Du et al. [62] found that the activation energy fell from 145 to 120 kJ mol^{-1} with addition of 2% calcium as catalyst. At the same time the ratio of CO to CO_2 fell from unity to 0.01 at 663 K. Ciambelli et al. [112] also found that the action of a potassium–copper–vanadium catalyst promoted CO_2 formation ($CO/CO_2 \sim 0.05$). They propose that the catalyst promotes the formation of surface oxygen complexes with relatively low activation energies for desorption.

The catalyst generally lowers activation energy, typically by 30–80 kJ mol^{-1}, that is from 170 to 120 [38] and 151 to 100 kJ mol^{-1} [69]. Since the uncatalysed activation energies are generally higher, the rates will overtake the catalysed rate as temperature rises. Above the crossover temperature, the rates will be identical.

The order of the oxidation reaction with CuO catalyst is reported by de Soete [38] as unity. The measurement of the rates of the reaction stages indicates that catalytic combustion, like the uncatalysed system, is controlled by the adsorption of the gaseous oxidiser. This should be contrasted with Ciambelli et al. [112] who identify desorption as the controlling step. However, higher desorption temperatures (up to 1000°C) were studied [69], whereas de Soete's data refer to lower temperatures (Fig. 2).

Neri et al. [67] discuss oxygen spillover for catalysts containing platinum group metals. They found a good correlation between catalyst reactivity and the enthalpy of formation of the metal oxides. They proposes that lattice oxygen acts in a redox manner, consistent with the findings of McKee for graphite [121]. This implies an oxygen 'spillover' effect from the noble metal promoter, and requires good contact between the carbon and catalyst. During catalyst studies with Cu–V–K, Ciambelli et al. [39] report that significant oxidation of carbon black took place even in the absence of oxygen, indicating that a redox mechanism was active.

Ciambelli et al. [69] found that during the combustion of uncatalysed soot the order was 0.8 at 593 K, but 0.5 when catalysed with Cu–V–K. This is explained by proposing a redox or oxygen 'shuttle' mechanism. The reaction mechanism consists of dissociative adsorption of oxygen onto the catalyst surface (oxidative step), followed by carbon oxidation by the oxygen of the catalyst (reductive step). If the oxidative step is in equilibrium and the reductive step is rate-limiting, the order should be 0.5.

For loose contact with metal oxides, a correlation between melting temperature (and hence partial pressure) and catalyst efficiency was noted by Neeft [109], Ahlstrom [117], Neri [67] and McKee [121]. Migration across the carbon surface is considered to be the mechanism involved. Mul et al. [115] note that $CuCl_2$ is able to 'wet' alumina and speculates that it will spread across carbon as well.

Metals such as copper can be promoted by the addition of a promoter such as potassium [69], molybdenum [115], niobium [122], iron as spinel [123], vanadium [67,119] or chlorine [104].

McKee addressed the mechanism of graphite oxidation when catalysed by alkali metals [121,124]. The most effective species were the carbonates, oxides and hydroxides; other active salts tend to convert to these under gasification conditions. There is a threshold concentration of alkali carbonate catalyst below which it exhibits no

activity [19]. Neeft et al. [80] found increases in reactivity of 3–5 orders of magnitude with alkali metals. The effectiveness is inversely dependent on the atomic mass of the alkali, being highest for caesium and lowest for lithium. The increases are attributed to the redistribution of catalyst.

The mechanisms of attack of catalyst particles on carbon, such as pitting of the graphite basal plane, edge recession and channeling are demonstrated in Marsh and Kuo [58].

6. Gasification with steam, carbon dioxide or nitrogen dioxide

Gasification of soots produced from aromatic (α-MN) and aliphatic (*n*-HD) hydrocarbons with water vapour and carbon dioxide was studied by de Soete [38] using the same techniques as for oxygen. There was negligible reaction with H_2O below 800 K and the major product at higher temperatures was CO (CO/CO_2 ratio ~9). The order of reaction with respect to H_2O was close to one. The gasification rates with carbon dioxide were lower than those with water vapour. The reaction order for CO_2 was again one, but the quantities of product CO and CO_2 were generally of the same order.

Otto et al. [29] report on the increase in soot surface areas during gasification with H_2O and CO_2, but give no other information. Typical Arrhenius data for the gasification of *n*-HD soot with H_2O and CO_2 [38] are shown for comparison on Fig. 4. The data are similar to those reported for petroleum coke reacted with steam by Harris and Smith [125]. In general, the trends in the reaction of soot with H_2O and CO_2 are similar to those with oxygen, but at a reduced rate of reaction.

A study with isotopic CO_2 by Kapteijn et al. [126] confirmed the presence of two types of desorbable oxygen complexes on the surface of activated carbon. The more reactive species is present in smaller quantities but contributes more to the CO desorption. The desorption transients are exponential in form and exhibit a range of activation energies.

Moulijn and Kapteijn [59] propose a unified theory, involving adjacent active sites. The reaction sequence suggested for CO_2 oxidation involves semi-quinone C(O) and carbonyl CC(O) species, the former involving slow reactions and the latter more active:

$$CO_2 + C_f \rightarrow CO + C(O)$$
$$CO_2 + CC(O) \rightarrow CO + C(O)(CO)$$
$$C(CO) \rightarrow CO + C_f$$
$$C(O) \rightarrow CO + C_f$$

They imply that other oxidants will follow similar paths, both involving slow and fast reaction steps. Additional steps are involved with different oxidants.

Otto and Shelef [127] showed that metals catalyse the carbon–steam reaction, using graphite and metals deposited from aqueous solutions. The action of water vapour on graphite when catalysed by alkaline earth metals is reported by McKee [128]. Ba and Sr were more active than Ca and Mg. A carbonate–oxide oxidation–reduction cycle is proposed.

Kapteijn et al. [129] investigated the reactivity of carbon dioxide with graphite using alkali metal carbonates as catalysts. The results were similar to those cited above for oxygen gasification with soot, namely Cs>Rb>K>Na>Li. They identify five distinguishable temperature regions during outgassing under TPD. As concluded earlier, two types of surface oxide species of differing stability are present.

The reactivity of nitrogen dioxide NO_2 towards soot is far greater than that of oxygen at low temperatures. This is demonstrated by Fig. 8 [130], which depicts the specific rates of oxidation by each at 500°C, at the same concentration (0.1%). Water acts as a catalyst for the C–NO_2 reaction, and oxygen is also active in promoting oxidation at temperatures below its usual range of activity. A kinetic expression involving temperature and the concentrations of NO_2, O_2 and H_2O has been derived [131].

Early interest in the C–NO_2 reaction focussed on atmospheric reduction of NO_2 by carbonaceous particles in the air, see Ref. [132] for examples. The temperatures employed in these investigations were mostly ambient but ranged to 200°C. Chemisorption takes place with surface species like C–NO_2, C–ONO and C–N–NO_2 being formed. Chugtai and co-workers [132,133] found that at temperatures below 200°C NO_2 reacts with *n*-hexane soot to form NO, which is then disproportionates to N_2O and NO_2. At the same time small amounts of CO and CO_2 are released. A dual-site mechanism was proposed for the reaction of NO_2.

For automotive applications, the continuously regenerating trap (CRT) [134] is based on the oxidation by NO_2 of the soot collected in a particulate filter in the temperature

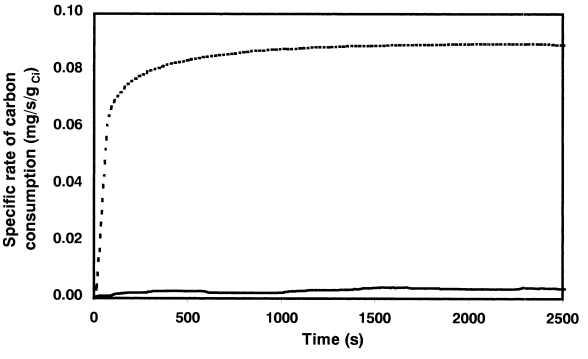

Fig. 8. Comparison of the specific oxidation rates of carbon black in fixed beds at 500°C for (—) 0.1% O_2 and (- - -) 0.1% NO_2 [130].

range 200–500°C. In this system NO_2 is produced by the oxidation of the NO in the engine exhaust by a catalyst in an upstream monolithic converter. Even though the rate of carbon consumption by NO_2 is small, it is enough to ensure an equilibrium in the particulate filter between the mass of soot produced by the engine and that consumed by the reaction.

The range of temperatures used by Lur'e and Mikhno [135] to investigate the gasification kinetics of graphitized soot by NO_2 was 100–350°C. The equipment employed was a fixed bed with a recirculating flow of reactant. The dominant reaction was:

$$C + 2NO_2 \rightarrow CO_2 + 2NO$$

but the presence of condensed surface products complicates the system. Small amounts of CO and N_2 are formed at higher temperatures. The order of reaction changes drastically with temperature, being unity above 300°C and rising to more than 2 as the temperature falls. A mechanism for the reaction based on the formation and subsequent decomposition of an intermediate species was proposed. The activation energy was found to be 50 kJ mol^{-1} in the temperature range 180–350°C.

Gray and Do [136,137] investigated gravimetrically the adsorption and reaction of NO_2 on an activated carbon (Norit RB) over a similar temperature range (150–350°C). At low temperatures (<100°C) the NO_2 is simply adsorbed but it undergoes reaction at higher temperatures. The surface reaction controls the overall kinetics, which are first order with respect to NO_2 at 300°C. When the random pore model was used to describe the evolution of surface area, the activation energy was found to be 86.2 kJ mol^{-1}. This is lower than those for O_2, H_2O and CO_2 gasification.

The extensive work of Tabor et al. [138] concerns the chemistry of the low temperature (ambient) interaction of NO_2 with three kinds of carbon, including carbon black. The major gaseous product in each case was NO, but the carbon product remained on the surface of the solid. At a temperature of 150°C, Yagud et al. [139] found that an activated charcoal produced CO_2 and NO according to the above equation.

The combustion behavior of the soot in a CRT system was investigated by Cooper and Thoss [140] on a test bench. The orders of reaction with respect to the NO_2 inlet concentration and to soot weight were found equal to 1. The benefit of the presence of water in the feed gas for soot oxidation was noted.

Enhanced activity of nitric oxide NO in the presence of water vapour as an oxidant for soot over Ce/Pt, Pt/SiO_2 and Cu/V/K/Cl/Ti catalysts has been demonstrated [141–143]. In each case the enhancement has been explained by the catalysed formation of NO_2 from the NO. The presence of SO_2 was found to further increase the rate [132,142].

7. Conclusion

Soots from various sources are structurally similar, and similar to commercial carbon blacks. The fundamental spherules are 20–30 nm in diameter, with little porosity. The four reactant gases O_2, CO_2, H_2O and NO_2 all oxidise and gasify soot, with NO_2 the most reactive at low temperatures. Two kinds of reactive site where adsorption intermediates are formed can be identified for the O_2 and NO_2 reactions. When the spherules are gasified, the extent of reactant penetration depends on the reactant and the temperature. In the absence of a flow-through gas supply, oxidation in beds depends on the supply of oxidant by diffusion to the interior. The reactivity towards oxygen is similar to that of other carbons on an area basis.

With catalyst present, the gasification mechanisms are modified, so that the reaction products, the activation energy and the apparent reaction order change. Two forms of catalyst addition have been identified, depending on the intimacy of contact. 'Tight' contact results in enhancement of the reaction rate for many metals, which may be less effective in 'loose' contact. Cerium and the noble metals are used for the control of diesel soot emissions. Alkali and alkaline earth metals are especially effective with H_2O and CO_2.

The control of soot emissions from automotive engines can now be achieved by installing filter monoliths in the exhaust line. These traps must be periodically regenerated by burning the deposited soot. This filtration device can be associated with the use of fuel additives to decrease the ignition temperature of the soot material by a catalytic effect.

Another technology, based on the continuous oxidation of soot by NO_2, is also a possible solution to meet the requirements regarding soot emissions by diesel engines. In that case NO_2 must be produced by a catalytic oxidation of NO before its reaction with the soot material trapped in a monolithic filter.

These technologies seem to be able to solve the problem of the soot emissions from automobile engines.

References

[1] McClure BT, Bagley ST, Gratz LD. The influence of an oxidation catalytic converter and fuel composition on the chemical and biological characteristics of diesel exhaust emissions, 1992, SAE paper 920854.

[2] Christensen R, Hansen MB, Schramm J, Binderup M-L, Jorgensen V. Mutagenic activity of the soluble organic fraction of exhaust gas particulate from a direct injection diesel engine, 1996, SAE paper 961977.

[3] Muhle H. Toxic and carcinogenic effects of fine particles — observations and hypotheses. In: International ETH workshop on nanoparticle measurement, Zurich: ETH, 1999, Paper 2.

[4] Haynes BS, Wagner HG. Soot formation. Prog Energy Combust Sci 1981;7:229–73.
[5] Lahaye J, Prado G. Morphology and internal structure of soot and carbon blacks. In: Siegla DC, Smith GW, editors, Particulate carbon formation during combustion, New York: Plenum Press, 1981.
[6] Smith OI. Fundamentals of soot formation in flames with application to diesel engine emissions. Prog Energy Combust Sci 1981;7:275–91.
[7] Donnet J-B. Fifty years of research and progress on carbon black. In: Second international conference on carbon black (Mulhouse), 1993, pp. 1–10.
[8] Bockhorn H, editor, Soot formation in combustion: mechanisms and models, Berlin: Springer, 1994.
[9] Murphy MJ, Hillenbrand LJ, Trayser DA, Wasser JH. Assessment of diesel particulate control — direct and catalytic oxidation, 1981, SAE paper 810112.
[10] Glassman I, Nishida O, Sidebotham G. Critical temperatures of soot formation. In: Bockhorn H, editor, Soot formation in combustion: mechanisms and models, Berlin: Springer, 1994, pp. 316–24.
[11] Hall-Roberts VJ, Hayhurst AN, Knight DE, Taylor SG. The origin of soot in flames: Is the nucleus an ion? Combust Flame 2000;120:578.
[12] Frenklach M. Surface growth mechanism of soot particles. In: Twenty-sixth international symposium on combustion, Philadelphia: The Combustion Institute, 1996, pp. 2285–93.
[13] Krestinin AV. Detailed modeling of soot formation in hydrocarbon pyrolysis. Combust Flame 2000;121:513–24.
[14] Veranth JM, Fletcher TH, Pershing DW, Sarofim AF. Measurement of soot and char in pulverised coal fly ash. Fuel 2000;79:1067–75.
[15] Lahaye J, Boehm P, Chambrion P, Ehrburger P. Influence of cerium oxide on the formation and oxidation of soot. Combust Flame 1996;104:199–207.
[16] Marcucilli F, Gilot P, Stanmore BR, Prado G. Experimental and theoretical study of diesel soot reactivity. In: Twenty-fifth international symposium on combustion, Philadelphia: The Combustion Institute, 1994, pp. 619–26.
[17] Neeft JPA, Nijhuis TX, Smakman E, Makkee M, Moulijn JA. Kinetics of the oxidation of diesel soot. Fuel 1997;76(12):1129–36.
[18] Walker PL, Austin LG, Nandi SP. In: Walker PL, editor, Chemistry and physics of carbon, vols. 1 and 2, New York: Marcel Dekker, 1966.
[19] Ahlström AF, Odenbrand CUI. Combustion characteristics of soot deposits from diesel engines. Carbon 1989;27:475–83.
[20] Courcot D, Abi-Aad E, Capelle S, Aboukaïs A. Preparation and characterisation of copper–cerium oxide catalysts and their application to the combustion of diesel soot. In: CaPOC 4, Brussels, 1997, pp. 303–12.
[21] Neeft JPA, Makkee M, Moulijn JA. Diesel particulate emission control. Fuel Proc Technol 1996;47:1–69.
[22] Zinbo M, Skewes LM, Hunter CE, Schuetzle D. Thermogravimetry of filter-borne diesel particulates. Thermochim Acta 1990;166:267–75.
[23] Heywood JB. Internal combustion engine fundamentals, New York: McGraw Hill, 1990.
[24] Farrauto RJ, Voss KE. Monolithic diesel oxidation catalysts. Appl Catal B 1996;10:29–51.
[25] Neoh KG, Howard JB, Sarofim AF. Effect of oxidation on the physical structure of soot. In: Twentieth international symposium on combustion, Pittsburgh: The Combustion Institute, 1984, pp. 951–7.
[26] Darmstadt H, Roy C, Donnelly PJ. Comparative investigation of defects on carbon black surfaces by nitrogen adsorption and SIMS. In: Third international conference on carbon black (Mulhouse), 2000, pp. 77–9.
[27] Ishiguro T, Suzuki N, Fujitani Y, Morimoto H. Microstructural changes of diesel soot during oxidation. Combust Flame 1991;85:1–6.
[28] Göritz D, Weigert A, Raab H. Investigation of the localisation of active sites on the surface of carbon black by scanning tunneling microscopy. In: Third international conference on carbon black (Mulhouse), 2000, pp. 43–50.
[29] Otto K, Sieg MH, Zinbo M, Bartosiewicz L. The oxidation of soot deposits from diesel engines, 1981, SAE paper 800336.
[30] Yuan S, Mériaudeau P, Perrichon V. Catalytic combustion of diesel soot particles on copper catalysts supported on TiO_2. Effect of potassium promoter on the activity. Appl Catal B 1994;3:319–33.
[31] Stoeckli F, Guillot A, Slasli A, Hugi-Cleary D. Microporosity in carbon blacks. In: Third international conference on carbon black (Mulhouse), 2000, pp. 67–75.
[32] Buczek B, Swiatkowski A, Zietek P, Trznadel BJ. Adsorption properties and porous structure within granules of activated carbons with different burnoff. Fuel 2000;79(10):1247–53.
[33] Brilhac J-F, Bensouda F, Gilot P, Brillard A, Stanmore B. Experimental and theoretical study of oxygen diffusion within packed beds of carbon black. Carbon 2000;38:1011–9.
[34] Lahaye J, Ehrburger-Dolle F. Mechanisms of carbon black formation. Correlation with morphology of aggregates. In: Second international conference on carbon black (Mulhouse), 1993, pp. 11–22.
[35] Noirot R, Gilot P, Gadiou R, Prado G. Control of soot emission by filtration and post-combustion. A laboratory study of the regeneration of an organic particulate trap assisted by hydrocarbon injection. Combust Sci Technol 1994;95:139–60.
[36] Smith IW. The combustion rate of coal chars: a review. In: Nineteenth international symposium on combustion, Philadelphia: The Combustion Institute, 1982, pp. 1045–65.
[37] Walker PL, Rusinko Jr F, Austin LG. Gas reactions of carbon. Adv Catal 1959;11:133.
[38] de Soete G. Catalysis of soot combustion by metal oxides. In: Western States section meeting, Salt Lake City, 21–22 March, The Combustion Institute, 1988.
[39] Ciambelli P, Corbo P, Parrella P, Scialo M, Vaccaro S. Catalytic oxidation of soot from diesel exhaust gases. 1. Screening of metal oxide catalysts by TG-DTG-DTA analysis. Thermochim Acta 1990;162:83–9.
[40] Ma J, Fang M, Li P, Zhu B, Lu X, Lau NT. Microwave-assisted catalytic combustion of diesel soot. Appl Catal A 1997;159:211–28.
[41] Stanmore BR. Use of the differential thermal gravimetric analyser for carbon/oxygen reactivity measurement. Fuel 1991;70:1485–7.

[42] Gilot P, Bonnefoy F, Marcucilli F, Prado G. Determination of kinetic data for soot oxidation. Modeling of competition between oxygen diffusion and reaction during thermogravimetric analysis. Combust Flame 1993;95:87–100.
[43] Stanmore B, Gilot P, Prado G. The influence of mass transfer in DTG combustion tests. Thermochim Acta 1994;240:79–89.
[44] Stanmore BR, Gilot P. The influence of sample containment on the thermogravimetric measurement of carbon black reactivity. Thermochim Acta 1995;261:151–64.
[45] Gilot P, Brillard A, Stanmore BR. Geometric effects on mass transfer during thermogravimetric analysis: application to the reactivity of diesel soot. Combust Flame 1995;102:471–80.
[46] Murphy MJ, Hillenbrand LJ, Trayser DA, Wasser JH. Assessment of diesel particulate control — direct and catalytic oxidation, 1981, SAE paper 810112.
[47] Herz RK, Sinkevitch RM. Reactors for investigation of soot combustion on filter surfaces. Carbon 1986;4:457–62.
[48] Vonarb R. PhD thesis, Université de Haute Alsace, 1999.
[49] Petersen RC. The oxidation rate of diesel particles which contain lead, 1987, SAE paper 870628.
[50] Lee KB, Thring MW, Beér JM. On the rate of combustion of soot in a laminar soot flame. Combust Flame 1962;6:137–45.
[51] Garo A, Prado G, Lahaye J. Chemical aspects of soot particles radiation in a laminar methane–air diffusion flame. Combust Flame 1990;79:226–33.
[52] Park C, Appleton JP. Shock-tube measurements of soot oxidation rates. Combust Flame 1973;20:369–79.
[53] Roth P, Brandt O, von Gersum S. High temperature oxidation of suspended soot particles verified by CO and CO_2 measurements. In: Twenty-third international symposium on combustion, Pittsburgh: The Combustion Institute, 1990, pp. 1485–91.
[54] Cavaliere A, Barbella R, Ciajolo A, D'Anna A, Ragucci R. Fuel and soot oxidation in diesel-like conditions. In: Twenty-fifth international symposium on combustion, Philadelphia: The Combustion Institute, 1994, pp. 167–74.
[55] Roth P, Eckhardt T, Franz B, Patschull J. H_2O_2-assisted regeneration of diesel particulate traps at typical exhaust gas temperatures. Combust Flame 1998;115:28–37.
[56] Ismail IMK, Walker Jr. PL. Detection of low temperature carbon gasification using DSC and TGA. Carbon 1989;27:549–59.
[57] Lear AE, Brown TC, Haynes BS. Formation of metastable oxide complexes during the oxidation of carbons at low temperatures. In: Twenty-third international symposium on combustion, Pittsburgh: The Combustion Institute, 1990, pp. 1191–7.
[58] Marsh H, Kuo K. Kinetics and catalysis of carbon gasification. In: Marsh H, editor, Introduction to carbon science, London: Butterworths, 1989, p. 107.
[59] Moulijn JA, Kapteijn F. Towards a unified theory of reactions of carbon with oxygen-containing molecules. Carbon 1995;33:1155–65.
[60] Kapteijn F, Meijer R, Moulijn JA, Cazorla-Amorós D. On why do different carbons show different gasification rates: a transient isotopic CO_2 gasification study. Carbon 1994;32:1223–31.
[61] Ahmed S, Back MH, Roscoe JM. A kinetic model for the low temperature oxidation of carbon. Combust Flame 1987;70:1–16.
[62] Du Z, Sarofim AF, Longwell JP. Activation energy in temperature-programmed desorption: Modeling and application to the soot-oxygen system. Energy Fuels 1990;4:296–302.
[63] Du Z, Sarofim AF, Longwell JP, Mims CA. Kinetic measurement and modelling of carbon oxidation. Energy Fuels 1991;5:214–21.
[64] Stanmore B, Brilhac J-F, Gilot P. The ignition and combustion of cerium-doped diesel soot, 1999, SAE paper 1999-01-0115.
[65] Querini CA, Ulla MA, Requejo F, Soria J, Sedrán UA, Miro EE. Catalytic combustion of diesel soot particles. Activity and characterisation of Co/MgO and Co, K/MgO catalysts. Appl Catal B 1998;15:5–19.
[66] Ma MC, Haynes BS. Surface heterogeneity in the formation and decomposition of carbon surface sites. In: Twenty-sixth international symposium on combustion, Philadelphia: The Combustion Institute, 1996, pp. 3119–25.
[67] Neri G, Bonaccorsi L, Donato A, Milone C, Musolino MG, Visco AM. Catalytic combustion of diesel soot over metal oxide catalysts. Appl Catal B 1997;11:217–31.
[68] Essenhigh RH. An integration path for the carbon–oxygen reaction with internal reaction. In: Twenty-second international symposium on combustion, Pittsburgh: The Combustion Institute, 1988, pp. 89–96.
[69] Ciambelli P, d'Amore M, Palma V, Vaccaro S. Catalytic combustion of an amorphous carbon black. Combust Flame 1994;99:413–21.
[70] Essenhigh RH. Influence of the initial particle density on the reaction mode of porous carbon particles. Combust Flame 1994;99:269–79.
[71] Nagle J, Strickland-Constable RF, editors, Fifth conference on carbon, London: Pergamon Press, 1962, p. 154.
[72] McCabe RW, Sinkevitch RM. A laboratory combustion study of diesel particulates containing metal additives, 1986, SAE technical paper no. 860011.
[73] Miyamoto N, Hou Z, Ogawa H. SAE paper 881224, 1988.
[74] Ciambelli P, Palma V, Russo P, Vaccaro S. Catalytic ceramic filter for diesel soot removal: preliminary investigations. In: CaPOC 4, Brussels, 1997, pp. 313–21.
[75] Smith IW. The intrinsic reactivity of carbons to oxygen. Fuel 1978;57:409.
[76] Leung KM, Lindsedt RP, Jones WP. A simplified reaction mechanism for soot formation in non-premixed flames. Combust Flame 1991;87:289–305.
[77] Gavalas GR. A random pore model with application to char gasification at chemically controlled rates. Am Inst Chem Eng J 1980;30:967–73.
[78] Radovic LR, Walker Jr PL, Jenkins RG. Importance of carbon active sites in the gasification of coal chars. Fuel 1983;62:849–56.
[79] Aarna I, Suuberg EM. Changes in reactive surface area and porosity during char oxidation. In: Twenty-seventh international symposium on combustion, Philadelphia: The Combustion Institute, 1998, pp. 2933–9.
[80] Neeft JPA, Makkee M, Moulijn JA. Catalytic oxidation of carbon black. I. Activity of catalysts and classification of oxidation profiles. Fuel 1998;77(3):111–9.
[81] Walker PL, Taylor RL, Ranish JM. An update on the carbon–oxygen reaction. Carbon 1991;29:411–21.
[82] Neeft JPA, Hoonaert F, Makkee M, Moulijn JA. The effects of heat and mass transfer in thermogravimetrical analysis. A

case study towards the catalytic oxidation of soot. Thermochim Acta 1996;287:261–78.
[83] Gilot P, Marcucilli F, Prado G. Porous media and the use of thermobalances: the kinetics of combustion processes. In: Nickel KG, editor, Corrosion of advanced ceramics, Amsterdam: Kluwer, 1994, p. 329.
[84] Bhatia SK, Perlmutter DD. A random pore model for fluid–solid reactions. I. Isothermal, kinetic control. Am Inst Chem Eng J 1980;26:379–86.
[85] Simon GM, Stark TL. Diesel particulate trap regeneration using ceramic wall-flow traps, fuel additives, and supplemental electric lighters, 1985, SAE paper 850016.
[86] Tan JC, Opris CN, Baumgard KJ, Johnson JH. A study of the regeneration process in diesel particulate traps using a copper fuel additive, 1996, SAE paper 960136.
[87] Lepperhof G, Lüders H, Barthe P, Lemaire J. Quasi-continuous particle trap regeneration by cerium additives, 1995, SAE paper 950369.
[88] Lepperhof G. Soot formation and oxidation in IDI and DI diesel engines, SIA, 1990, pp. 55–61.
[89] Golothan DW. Diesel engine exhaust smoke: the influence of fuel properties and the effects of using barium-containing fuel additive, 1967, SAE paper 670092.
[90] Wiedemann B, Neumann KH. Vehicular experience with additives for regeneration of ceramic diesel filters, 1985, SAE paper 850017.
[91] Ise H, Saitoh K, Kawagoe M, Nakayama O. Combustion modes of light duty diesel particulates in ceramic filters with fuel additives, 1986, SAE paper 860292.
[92] Lawson A, Vergeer HC, Drummond W, Mogan JP, Dainty ED. Performance of a ceramic diesel particulate trap over typical mining duty cycles using fuel additives, 1985, SAE paper 850150.
[93] Gantawar AK, Opris CN, Johnson JH. A study of the regeneration characteristics of silicon carbide and cordierite diesel particulate filters using a copper fuel additive, 1997, SAE paper 970187.
[94] Konstandopoulos AG, Gratz LD, Johnson JH, Bagley ST, Leddy DG. Ceramic particulate traps for diesel emissions control: effects of a manganese–copper fuel additive, 1988, SAE paper 880009.
[95] Dementhon JB, Martin B, Richards P, Rush M, Williams D, Bergonzini L, Morelli P. Novel additive for particulate trap regeneration, 1995, SAE paper 952355.
[96] Wade WR, White JE, Florek JJ, Cikanek HA. Thermal and catalytic regeneration of diesel particulate traps, 1983, SAE paper 830083.
[97] Levin MD, Koehler DE, Saile JA. Copper fuel additives as a part of a particulate emission control strategy, 1990, SAE paper 901619.
[98] Saito T, Nabetani M. Surveying tests of diesel smoke suppression with fuel additives, 1973, SAE paper 730170.
[99] Pattas KN, Michalopoulou CC. Catalytic activity in the regeneration of the ceramic diesel particulate trap, 1992, SAE paper 920362.
[100] Pattas KN, Samaras Z, Roumbos A, Lemaire J, Mustel W, Rouveirolles P. Regeneration of DPF at low temperatures with the use of a cerium based fuel additive, 1996, SAE paper 960135.
[101] Pattas KN, Kyriakis N, Samaras Z, Manikas T, Mihailidis A, Mustel W, Rouveirolles P. The behaviour of metal DPFs at low temperatures in conjunction with a cerium based additive, 1998, SAE paper 980543.
[102] Bonnefoy F, Gilot P, Stanmore BR, Prado G. A comparative study of carbon black and diesel soot reactivity in the temperature range 500–600°C; effect of additives. Carbon 1994;32:1333–40.
[103] Lahaye J, Boehm S, Ehrburger P. Metallic additives in soot formation and post-combustion. In: Bockhorn H, editor, Soot formation in combustion: mechanisms and models, Berlin: Springer, 1994, pp. 307–15.
[104] Mul G, Neeft JPA, Makkee Kapteijn F, Moulijn JA. Catalytic oxidation of model soot by chlorine based catalyst. In: CaPOC 4, Brussels, 1997, pp. 323–32.
[105] Solvat O, Marez P, Belot G. Passenger car serial application of a particulate filter system on a common rail direct injection diesel engine, 2000, SAE paper 2000-01-0473.
[106] Voss KE, Lampert JK, Farrauto RJ, Rice GW, Punke A, Krohn R. Catalytic oxidation of diesel particulates with base metal oxides. In: CaPOC 3, Brussels (April), 1994, pp. 227–41.
[107] Farrauto RJ, Voss KE. Monolithic diesel oxidation catalysts. Appl Catal B 1996;10:29–51.
[108] Neeft JPA, van Pruissen OP, Makkee M, Moulijn JA. Catalytic oxidation of diesel soot: catalyst development. In: CaPOC 3, Brussels (April), 1994, pp. 355–64.
[109] Neeft JPA, Makkee M, Moulijn JA. Catalysts for the oxidation of soot from diesel exhaust gases. I. An exploratory study. Appl Catal B 1996;8:57–78.
[110] Neeft JPA, van Pruissen OP, Makkee M, Moulijn JA. Catalysts for the oxidation of soot from diesel exhaust gases. II. Contact between soot and catalyst under practical conditions. Appl Catal B 1997;12:21–31.
[111] Ciambelli P, D'Amore M, Palma V. Catalytic combustion of carbon particulate at high values of the carbon/catalyst mass ratio. In: Twenty-sixth international symposium on combustion, Philadelphia: The Combustion Institute, 1996, pp. 1789–96.
[112] Ciambelli P, Di Pietro A, Palma V, Vaccaro S. Characterisation of the catalytic oxidation of carbon black by TPD. Thermochim Acta 1993;227:19–26.
[113] Ciambelli P, Palma V, Vaccaro S. Low temperature carbon particulate oxidation on a supported Cu/V/K catalyst. Catal Today 1993;17:71–8.
[114] McKee DW. Metal oxides as catalysts for the oxidation of graphite. Carbon 1970;8:623–35.
[115] Mul G, Neeft JPA, Kapteijn F, Makkee M, Moulijn JA. Soot oxidation catalysed by a Cu/K/Mo/Cl catalyst: Evaluation of the chemistry and performance of the catalyst. Appl Catal B 1995;6:339–52.
[116] Setzer C, Schütz W, Schüth F. Transition metal compound oxide catalysts for lowering the light-off temperature of particles from diesel exhaust. In: Proceedings 10th international congress on catalysis, Budapest, Hungary, Amsterdam: Elsevier, 1993, pp. 2629–32.
[117] Ahlström AF, Odenbrand CUI. Catalytic combustion of soot deposits from diesel engines. Appl Catal 1990;60:143–56.
[118] Ahlström AF, Odenbrand CUI. Combustion of soot deposits from diesel engines on mixed oxides of vanadium pentoxide and cupric oxide. Appl Catal 1990;60:157–72.
[119] Badini C, Saracco G, Serra V. Combustion of carbonaceous

materials by Cu–K–V based catalysts. I. Role of copper and potassium vanadates. Appl Catal B 1997;11:307–28.
[120] Badini C, Serra V, Saracco G, Montorsi M. Thermal stability of Cu–K–V catalyst for diesel soot combustion. Catal Lett 1996;37:247–54.
[121] McKee DW. Mechanisms of the alkali metal catalysed gasification of carbon. Fuel 1983;62:170–5.
[122] Bellaloui A, Varloud J, Mériaudeau P, Perrichon V, Lox E, Chevrier M, Gauthier C, Mathis F. Low temperature diesel soots combustion using copper based catalysts modified by niobium and potassium promoters. Catal Today 1996;29:421–5.
[123] Shangguan WF, Teraoka Y, Kagawa S. Simultaneous removal of NO_x and diesel soot particulates over ternary AB_2O_4 spinel-type oxides. Appl Catal B 1996;8:217–27.
[124] McKee DW, Chatterji D. The catalytic behaviour of alkali metal carbonates and oxides in graphite oxidation reactions. Carbon 1975;13:381–90.
[125] Harris DJ, Smith IW. In: Twenty-third international symposium on combustion, Philadelphia: The Combustion Institute, 1990, p. 1185.
[126] Kapteijn F, Meijer R, Moulijn JA, Cazorla-Amorós D. On why do different carbons show different gasification rates: a transient isotopic CO_2 gasification study. Carbon 1994;32:1223–31.
[127] Otto K, Shelef M. Effects of selected catalysts on kinetic parameters of the carbon–steam reaction. Chem Eng Commun 1980;5:223–32.
[128] McKee DW. Catalysis of the graphite–water vapour reaction by alkaline earth salts. Carbon 1979;17:419–25.
[129] Kapteijn F, Abbel G, Moulijn JA. CO_2 gasification of carbon catalysed by alkali metals. Fuel 1994;63:1036–42.
[130] Jacquot F, Logie V, Brilhac JF, Gilot P. Comparison of soot reactivity in the presence of oxygen or NO_2. In: Nanoparticle Congress of ETH, Zurich, 2000, August.
[131] Jacquot F, Logie V, Brilhac JF, Gilot P. Kinetics of the oxidation of carbon black by NO_2: influence of the presence of water and oxygen. Carbon 2001: in press.
[132] Chugtai AR, Welch WF, Akhter MS, Smith DM. A spectroscopic study of gaseous products of soot — oxides of nitrogen/water reactions. Appl Spectosc 1990;44:294–8.
[133] Chugtai AR, Gordon SA, Smith DM. Kinetics of the hexane soot reaction with NO_2/N_2O_4 at low concentration. Carbon 1994;32:405–16.
[134] Cooper BJ, Radnor HJ, Jung W, Thoss JE. Treatment of diesel exhaust gases. US patent 4,902,487 (1990).
[135] Lur'e BA, Mikhno AV. Interaction of NO_2 with soot. Kinet Catal 1997;38:490–7.
[136] Gray PG, Do DD. Modelling the interaction of nitrogen dioxide with activated carbon. I. Adsorption dynamics at a single particle. Chem Eng Commun 1992;117:219–40.
[137] Gray PG, Do DD. Modelling the interaction of nitrogen dioxide with activated carbon. II. Kinetics of reaction with pore evolution. Chem Eng Commun 1993;118:333–42.
[138] Tabor K, Gutzwiller L, Rossi MJ. Heterogeneous chemical kinetics of NO_2 on amorphous carbon at ambient temperature. J Phys Chem 1994;98:6172–86.
[139] Yagud BY, Amirova SA, Kefer RG. The reaction of nitrogen dioxide and nitrosyl chloride with activated charcoal. Russ J Inorg Chem 1971;16:792–4.
[140] Cooper BJ, Thoss JE. SAE paper 890404, 1989.
[141] Jelles SJ, Makkee M, Moulijn JA, Acres GJK, Peter-Hoblyn JD. Diesel particulate control. Application of an activated particulate trap in combination with fuel additives at an ultra low dose rate, 1999, SAE paper 1999-01-0113.
[142] Oi-Uchisawa J, Obuchi A, Ogata A, Enomoto R, Kushiyama S. Effect of feed gas composition on the rate of carbon oxidation with Pt/SiO_2 and the oxidation mechanism. Appl Catal B 1999;21:9–17.
[143] Ciambelli P, Palma V, Russo P, Vaccaro S. The role of No in the regeneration of catalytic ceramic filters for soot removal from exhaust gases. Catal Today 2000;60:43–9.